THE PENNSYLVANIA
STATE UNIVERSITY

IONOSPHERIC RESEARCH

Scientific Report No. 235

UNPUBLISHED PRELIMINARY DATA

SATELLITE STUDIES OF THE DISTRIBUTION OF IONIZATION ACROSS THE MAGNETIC EQUATOR

by
J. D. Kolesar

February 20, 1965

IONOSPHERE RESEARCH LABORATORY

University Park, Pennsylvania NASA Grant NsG-114-61

Ionospheric Research

NASA Grant NsG-114-61

Scientific Report

on

"Satellite Studies of the Distribution of Ionization Across the Magnetic Equator"

by

J. D. Kolesar

February 20, 1965

Scientific Report No. 235

Ionosphere Research Laboratory

Submitted by: W J Ross

W. J. Ross, Professor of Electrical Engineering

Approved by: G. H. Waynick

A. H. Waynick, Professor of Electrical Engineering.
Director, Ionosphere Research Laboratory

The Pennsylvania State University
College of Engineering
Department of Electrical Engineering

TABLE OF CONTENTS

ABSTRACT

15815

Several theories concerning the distribution of ionization about the magnetic equator under equilibrium conditions are discussed. The predictions are investigated experimentally using topside sounder satellite data and also total electron content data obtained from satellite beacon experiments.

It is found that the experimental data is in general agreement with an analytic model for the equatorial anomaly although there are departures in detail.

An equatorial trough in electron content is found to develop at about noon each day and persists into late evening. Following local magnetic disturbances the anomaly is less likely to be present.

Author

CHAPTER I - INTRODUCTION

A. The Ionosphere

Ionization in the upper atmosphere is produced by energetic radiation from the sun absorbed by constituents in the atmosphere. The ionization is subject to a number of physical and chemical reactions including, recombination, transfer of charge to other ions, and movement of ionization from the height at which it is produced by diffusion and other motions. Production and transport rates are very height dependent and often depend on the density of particular atmospheric gases. Consequently ionization seen at any one time and place in the ionosphere is not always simply related to the original ionization processes.

One very useful way of studying the distribution of ionization in the ionosphere has been by radio wave probing. Measurements are made of the dispersion in echo range of pulses radiated from a transmitter on the ground and reflected from the ionosphere. The reflection conditions are controlled principally by the electron distribution, and the data can be analyzed to give electron density vs height profiles. This method is applicable to the bottomside of the ionosphere. Above a certain critical

frequency, where the electron density is maximum, the radio waves penetrate the ionosphere and do not return to the earth. Measurements of this nature have been done extensively during the past three decades and have led to a general description of the bottomside ionosphere.

Since 1962 similar measurements have been done for the topside ionosphere using the "Alouette" topside sounder satellite. In principle the radio wave probing of the topside is identical to the bottomside technique. The Alouette satellite has yielded a large number of profiles for various places and times of day.

B. The Geomagnetic Anomaly

From the earlier soundings unusual behavior of the critical frequency near the equator was noted from mid-day to evening. Further study revealed that the behavior was associated with the magnetic equator, and that the critical frequency often had a trough of values at the magnetic equator relative to adjacent latitudes. Attempts to explain this phenomenon were evolved associating the horizontal magnetic field in this region with the anomaly, in particular by supposing that this horizontal field restricts the vertical diffusion

of ionization.

During the afternoon and evening period each day the anomaly is most pronounced, and at these times also changes in the ionization profiles are relatively slow. It is natural therefore to seek an explanation for the anomaly in terms of equilibrium models of the ionosphere.

The geomagnetic anomaly may be reviewed best from the variation of electron density with magnetic latitude at constant heights. Croom, Robbins and Thomas (1959) give a description for the bottomside ionosphere. Their results are shown in Fig. 1. The Alouette topside sounder results are shown in Fig. 2. As illustrated in these figures there is an increase in electron density away from the magnetic equator. The maximum value of N vs latitude moves towards the equator with increasing height. These angular peaks fall on a calculated magnetic field line. At low heights the anomaly disappears.

C. Historical Background of Anomaly

D. F. Martyn first reported the behavior of the F2 region over Huancayo as not conforming to the Chapman variation $(\cos x)^{1/2}$ where x is the solar zenith angle, E. Appleton (1947, 1950, 1954)

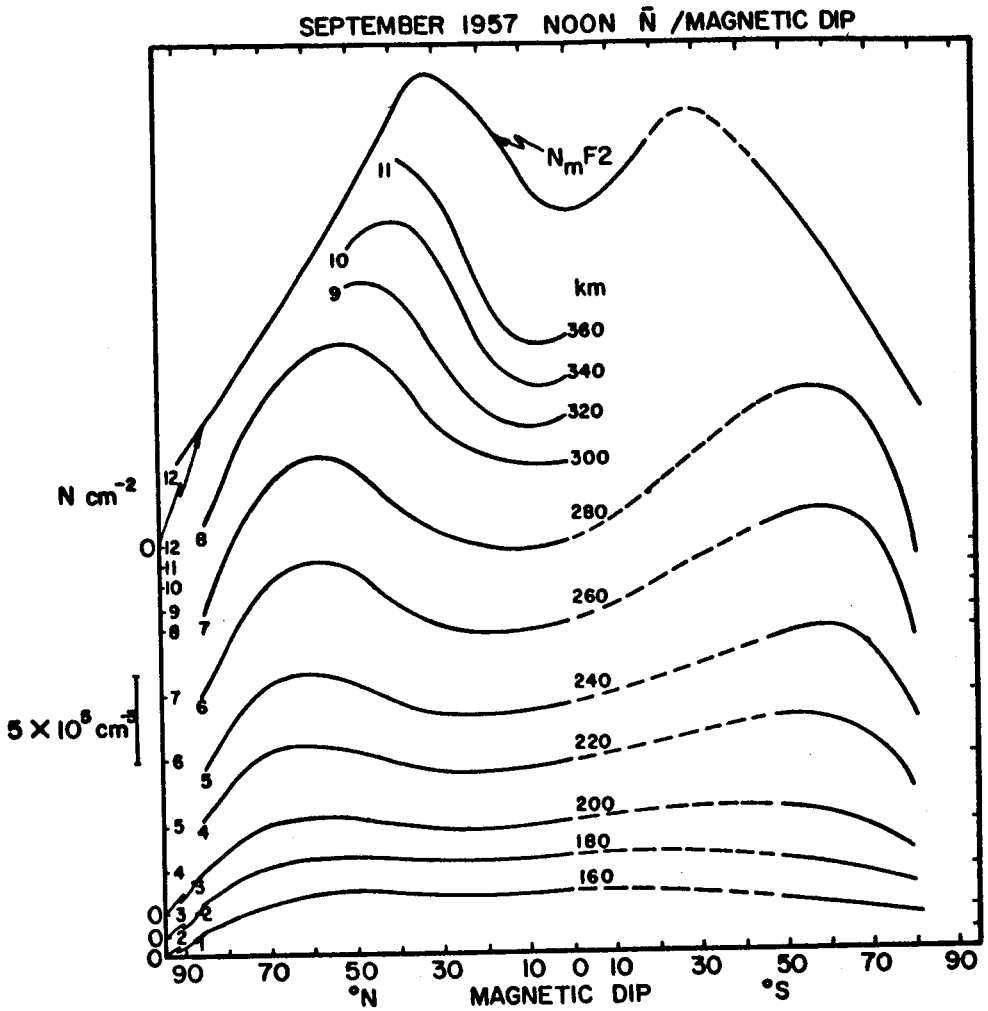

VARIATION OF ELECTRON DENSITY WITH MAGNETIC DIP AT DIFFERENT ALTITUDES FOR SEPTEMBER, 1957; AVERAGE PEAK ELECTRON DENSITY $N_m F2$ IS ALSO SHOWN. ALL VALUES ARE AVERAGED FOR NOON. THE ZERO OF THE SCALE FOR EACH HEIGHT IS MARKED.

FIGURE 1

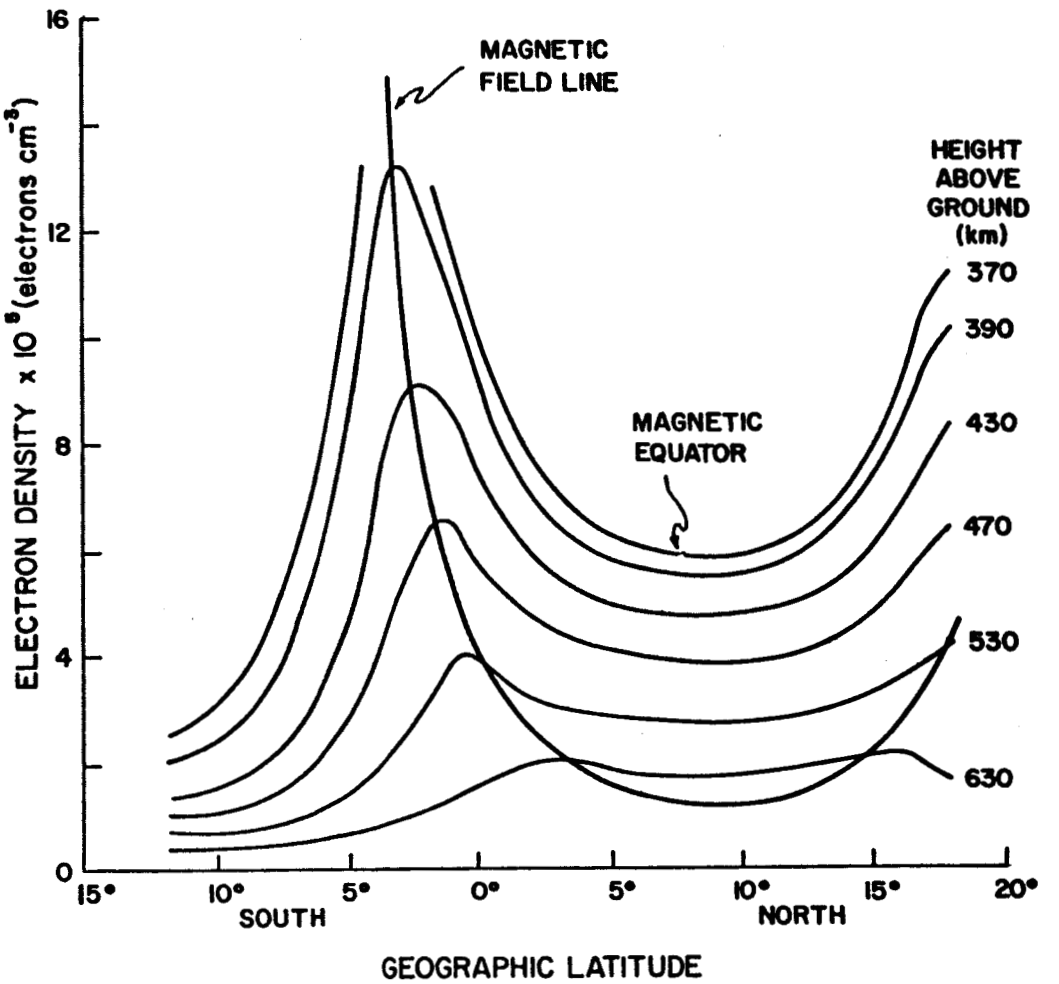

PLOTS SHOWING THE ELECTRON CONCENTRATION AT VARIOUS HEIGHTS ABOVE GROUND. SINGAPORE REV. 4762 13 SEPT. 1963 1248 L.M.T.

FIGURE 2

in a number of papers showed some of the features of the anomaly and in particular the variation of the critical frequency as being symmetrical about the magnetic equator. D. F. Martyn (1959) hypothesized that an upward lift of ionization at the equator coupled with diffusion would explain the geomagnetic anomaly and R. A. Duncan (1960) attempted to give a quantitative description using this approach. His calculations did not yield a realistic picture of the anomaly however. Goldberg and Schmerling (1962) showed that a constant or exponential electron density distribution along a field line produces effects similar to the anomaly.

The inclusion of diffusive movements along field lines in the theory has led to more elegant descriptions of the geomagnetic anomaly. Some of the major developments will be discussed more thoroughly in the next chapter.

D. Statement of the Problem

Experimental observations of the geomagnetic anomaly have led to theories attempting to explain this phenomenon. Some of these theories have not yielded physically realizable results. Goldberg and Schmerling (1963) have developed an approach whose results are generally in better

agreement with observation than those of previous workers. This theory was developed further by Goldberg et al. It is the purpose of this paper to analyze the existing theories and examine them in relation to available experimental data obtained from: 1) measurements of the total electron content variation with latitude over Huancayo, Peru, using satellite beacon methods, and 2) topside electron density profiles made from some Alouette topside sounder data over Singapore.

A study is also made of the behavior of the anomaly in total electron content during magnetically disturbed periods.

CHAPTER II - THEORIES AND RESULTS DESCRIBING THE GEOMAGNETIC ANOMALY

A. The Diffusion Operator

The equilibrium continuity equation for electrons is written symbolically as

$$(1)\quad \frac{\partial N}{\partial t} = -\mathrm{div}(Nv) + q - L = 0$$

where N is the electron density, -div(Nv) the diffusion term, and q and L the production and loss rates respectively. The geometry of the earth's magnetic field is incorporated in the diffusion term. A diffusion operator Ð may be defined as

$$(2)\quad -\mathrm{div}(Nv) = D\text{Ð}N$$

where D is the coefficient of diffusion.

P. C. Kendall (1962) has derived the form of the diffusion operator in a purely vectorial manner. A. J. Lyon (1963) derives the operator using a more physical approach which will be summarized here.

The basic assumptions of Kendall's and Lyon's derivations are:

a) Diffusion of ions and electrons is along the magnetic lines of force, and the relevant equation of motion for the ambipolar diffusion is for motions parallel to a line of force.

b) Isothermal atmosphere

c) Electrically neutral atmosphere, $N_e = N_i = N$

d) There is one type of ion only, of mass M_i, partial pressure $P_i = NkT$, $P_i = P_e$. P_e is the partial pressure of electrons

e) The mean motion of the ionization does not affect the mean motion of the neutral atmosphere.

f) The diffusion constant D is inversely proportional to n, the density of neutral atoms

g) A constant scale height $H = \frac{kT}{mg}$

m = mass of the ions, assumed to have the same mass of the atoms of the neutral gas.

g = acceleration of gravity

k = Boltzmann's constant

T = temperature

h) The magnetic field of the earth is described by a centered dipole model.

The geometry of Lyon's derivation is illustrated in Fig. 3 where

x = distance along a field line

ϕ = magnetic latitude

$d\lambda$ = element of longitude corresponding to dy

dy = element of distance normal to meridian plane

a = distance from the center of the earth

dl = element of distance in meridian plane normal

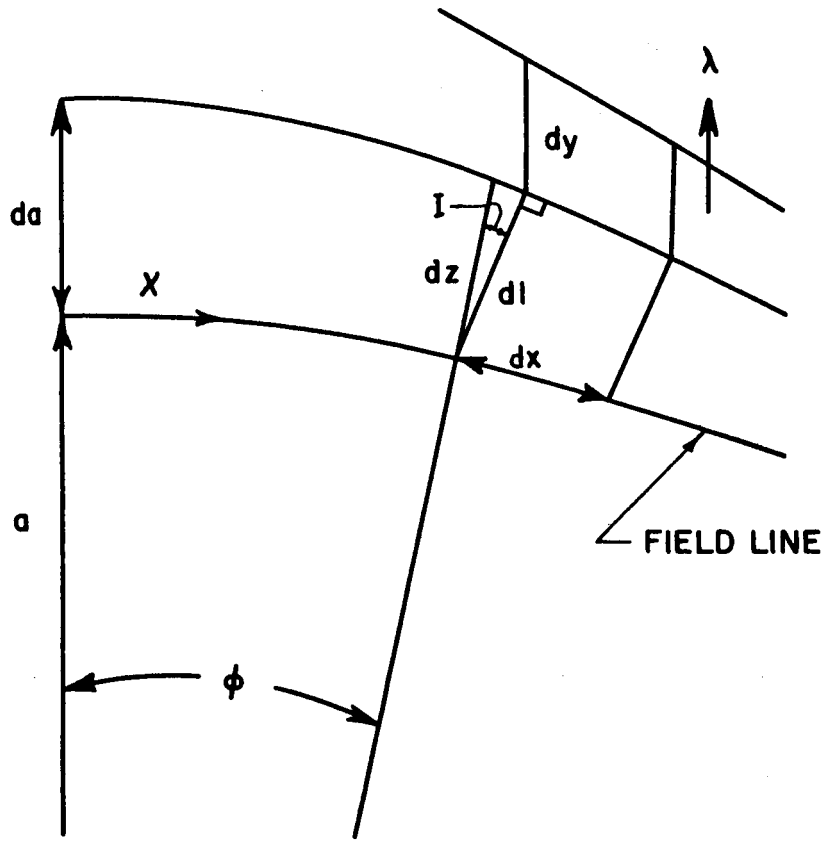

GEOMETRY OF TUBE OF FORCE

FIGURE 3

to field lines.

I = dip angle

The dipole field relation for a line of force is given by

$$(3) \quad r = a \cos^2 \phi$$

From the geometry in Fig. 3 and equation (3).

$$(4) \quad dl = dz \cos I = \cos^2 \phi \cos I \, da$$

$$(5) \quad dy = r \cos\phi \, d\lambda = a \cos^3 \phi \, d\lambda$$

Along a field line the force per particle and the mean velocity of diffusion are given by

$$(6) \quad F = -\frac{kT}{NH} \frac{dN}{dx} + mg \sin I$$

$$(7) \quad v = \frac{F}{mbH} = -d_o \, e^c \left[\frac{1}{N} \frac{dN}{dx} - \tfrac{1}{2} \sin I \right]$$

where b = collision frequency with neutral molecules

c = height at points along a field line measured in units of H

d_o = diffusion rate

The rate of increase of ionization through an element along a tube of force is

$$(8) \quad \text{Þ}N = -\text{div}(Nv) = -\frac{\frac{d}{dx}(Nv \, dy \, dl) \, dx}{dy \, dl \, dx}$$

Using equations (4), (5), (7), (8) results in

$$(9) \quad \text{Þ}N = -\text{div}(Nv) = d_o e^c \left[\frac{d^2N}{dx^2} - \frac{3}{2} \sin I \frac{dN}{dx} \right.$$

$$- \frac{(9 + 15 \sin^2\phi)}{a \cos^2\phi\ (1 + 3 \sin^2\phi)} \frac{dN}{dx} + \frac{(15 \sin^4\phi + 10 \sin^2\phi - 1)}{a \cos^2\phi\ (1 + 3 \sin^2\phi)^2} N$$

$$+ \frac{N}{2} \sin^2 I \Bigg]$$

Equation (9) is the identical equation that Kendall derives in terms of arc length with the exception that here x represents the arc length measured from $\phi = 0$. In Kendall's derivation arc length is measured in the same sense of a unit vector pointing towards $\phi = 0$. This results in a sign change in $\frac{dN}{dx}$ between Lyon's and Kendall's derivations.

The form of equation (9) in terms of magnetic latitude is

$$(10) \quad d_o e^c H^2 \dot{N} = \frac{d_o e^c}{a^2 c^2 \sigma} \left[\frac{d^2 N}{d\phi^2} - \left(\frac{3s}{ac\sigma} \right. \right.$$

$$\left. \left. - \frac{s(11 + 9s^2)}{a^2 c^2 \sigma^2} \right) \frac{dN}{d\phi} + \left(\frac{2s^2}{\sigma} + \frac{15s^4 + 10s^2 - 1}{ac^2\sigma} \right) N \right]$$

where $s = \sin \phi$

$c = \cos \phi$

$\sigma = 1 + 3 \sin^2\phi$

a = the distance of the field line apogee from the center of the earth expressed in units of H

This is the form which has been used by others in numerically integrating the continuity equation.

B. Numerical Solutions of the Continuity Equation

Kendall (1963) has numerically integrated the equilibrium continuity equation using equation (10) and neglecting the term $\frac{15s^4 + 10s^2}{ac^2\sigma}$. The form of the loss term was taken as BN, where B is the linear recombination coefficient. Ratcliffe (1956) derived a form for the loss term from the predominant process of charge exchange followed by dissociative recombination. At heights in the region of interest here, the loss term may be approximated by BN. A Chapman form for overhead sun was used for the production term.

$$(11) \quad q = q_o \exp\left[1-z - \exp(-z)\right]$$

where z = height above the level of maximum production, measured in units of H.

The level of maximum production was taken at 180 km. The boundary conditions which were used were that N is symmetrical about the equator, and that N becomes zero when z is large and negative.

The important result this numerical integration yielded was that the increase in "N maximum" with latitude over approximately ten degrees was less than five per cent. This is in contrast with experimental observations showing an

increase of roughly fifty per cent. Kendall, on the basis of these calculations, concluded that diffusion alone could not account for the geomagnetic anomaly.

Rishbeth, Lyon and Peart (1963) have also numerically integrated the equilibrium continuity equation along field lines. The production term was taken as having an approximately mid-day equinoctial form.

(12) $q = q_o \exp(1-z-\sec \phi \exp(-z))$

Two forms were used for the loss term, one being BN, and the other $BN + \alpha N^2$ where the recombination coefficient was taken as

(13) $B = B_o \exp(-kz)$ and α is the radiative recombination coefficient. The value k in (13) was taken for two cases, $k = 1$ corresponding to an isothermal atmosphere where B has the same scale height as the ionizable gas, and $k = 2$ where B depends on the concentrations of molecular gas O_2, while the ionizable gas is O.

The conditions imposed were

a) N is symmetrical about the equator

b) $\frac{dN}{d\phi} = 0$ at $\phi = 0$

c) $N \rightarrow 0$ as $\phi \rightarrow 90^o$

The solution was found for a variety of values of parameters appearing in the continuity equation.

The results of these computations are similar to those of Kendall but somewhat more elaborate. First N as a function of latitude along a given line of force was computed. These curves exhibited a maximum N with latitude.

The increase in "N maximum" with latitude was roughly 10 per cent for k=1 and 5 per cent for k=2. The crests of "N maximum" were around 10 degrees magnetic latitude. Experimental observations shows these crests at about 15 to 20 degrees latitude.

The results did not alter appreciably when the radiative recombination term was added to the loss term.

Rishbeth, Lyon and Peart concluded that the process of diffusion along a field line is inadequate to account for the actual features of the equatorial ionosphere.

C. Recent Theories

Goldberg and Schmerling (1963) have proposed a theory explaining the geomagnetic anomaly. The assumptions on which the theory is based are

those used by Kendall. An additional assumption was made that production and loss are independent of magnetic latitude and a function of radial distance only. The resulting form of the diffusion term arrived at after solving the equations of motion of ions and electrons along field lines and some simplifying assumptions neglecting angular gradients of N is

$$(14)\quad \mathrm{div}(Nv) = -A \exp r/H_1 \left[\sin^2 I \frac{\partial^2 N}{\partial r^2} + \left(\sin^2 I \left(\frac{1}{H_1} + 2\frac{1}{H_2} \right) - \frac{2}{r} \right) \frac{\partial N}{\partial r} + \left(\frac{\sin^2 I}{2H_1 H_2} - \frac{1}{rH_2} \right) N \right]$$

where H_1 = scale height of neutral atoms

H_2 = scale height of ionizable constituent

r = radial height measured from the center of the earth.

A linear loss rate was assumed of the form

$$(15)\quad L = B(r)\ N(r,c)$$

The loss and diffusion terms were then placed into the equilibrium continuity equation and a power series solution was developed. The condition of symmetry of N with latitude was also invoked. The solution is then of the form

$$(16)\quad N(r, \phi) = \sum_{m=0}^{\infty} f_{2m}(r)\, \phi^{2m}$$

ϕ = magnetic latitude

A general recursion relation is then developed for the coefficients $f_{2m}(r)$. The important feature in Goldberg and Schmerling's work is the choice of a boundary condition. A Chapman profile is chosen for a radial distribution of ionization at the magnetic equator.

$$(17)\quad N(r,o) = f_o(r) = N(r_{max},o) \exp \tfrac{1}{2}\left[1 - k(r - r_m) - \exp(-k(r-r_m))\right]$$

$\frac{1}{k}$ = reciprocal scale length

This choice of a boundary condition provides the basic difference between this theory and those discussed previously. This choice of a boundary condition is of significant importance as will be seen later.

Goldberg and Schmerling pointed out that a parabolic profile also produced many features of the anomaly. The Chapman profile was chosen because it gave a fair approximation to the observed N-h profiles. Other authors were cited for support.

Production and loss are implicitly contained in this boundary condition. In the recursion relation

itself the difference between production and loss appeared as part of a coefficient. This term was set equal to zero in view of the fact that the production and loss effects in the boundary condition left a stronger effect on the resulting equations than do the appearance of the production and loss in the coefficients.

The general solution from equation (16) is then

$$(18)\quad N(r,\phi) = f_o + f_2\phi^2 + f_4\phi^4 + \dots$$

The first few coefficients are as follows using

$$(19)\quad F = \exp(-k(r-r_m))$$

$$(20)\quad f_o(r) = N_m F^{1/2} \exp\tfrac{1}{2}(1-F)$$

$$(21)\quad f_2(r) = \frac{rk}{2} f_o \left[F + \frac{1}{kH_2} - 1 \right]$$

$$(22)\quad f_4(r) = \frac{1}{8}(rk)^2 f_o \left[F^2 + 2\left(\frac{1}{kH_2} - 2\right) + \left(\frac{1}{kH_2} - 1\right)^2 \right]$$

Inclusion of the first two terms in equation (18) represents a small angle solution of parabolic form. This can describe the increase of N at constant height with latitude, but to resolve the angular peaks an additional term is needed. It was found that if $\frac{1}{kH_2} < 2$, f_4 was negative over

some height range. This was essential for a maximum of N to occur at some latitude.

The equations were numerically evaluated for N at constant heights as a function of magnetic latitude. Three cases were studied corresponding to high, intermediate and low sunspot numbers as shown in Fig. 4. For high sunspot number N has a maximum with latitude when f_4 is negative. The crests in N move towards the equator with increasing height. The troughs in N at constant heights are appreciable. These curves do represent the geomagnetic anomaly more realistically than the previously mentioned results. For intermediate and low sunspot numbers curves of N vs latitude have maximums at a range of heights between 400 and 500 km but at greater heights minima occurred instead. These extrema occur at roughly 10° in latitude. Further calculations including terms up to f_6 did not alter the features of the curves appreciably but the crests were resolved more completely with this higher order solution.

Finally the theory predicts an increase of "N maximum" with latitude of roughly fifty per cent for intermediate sunspot numbers. For high and low sunspot numbers the increase is appreciably greater

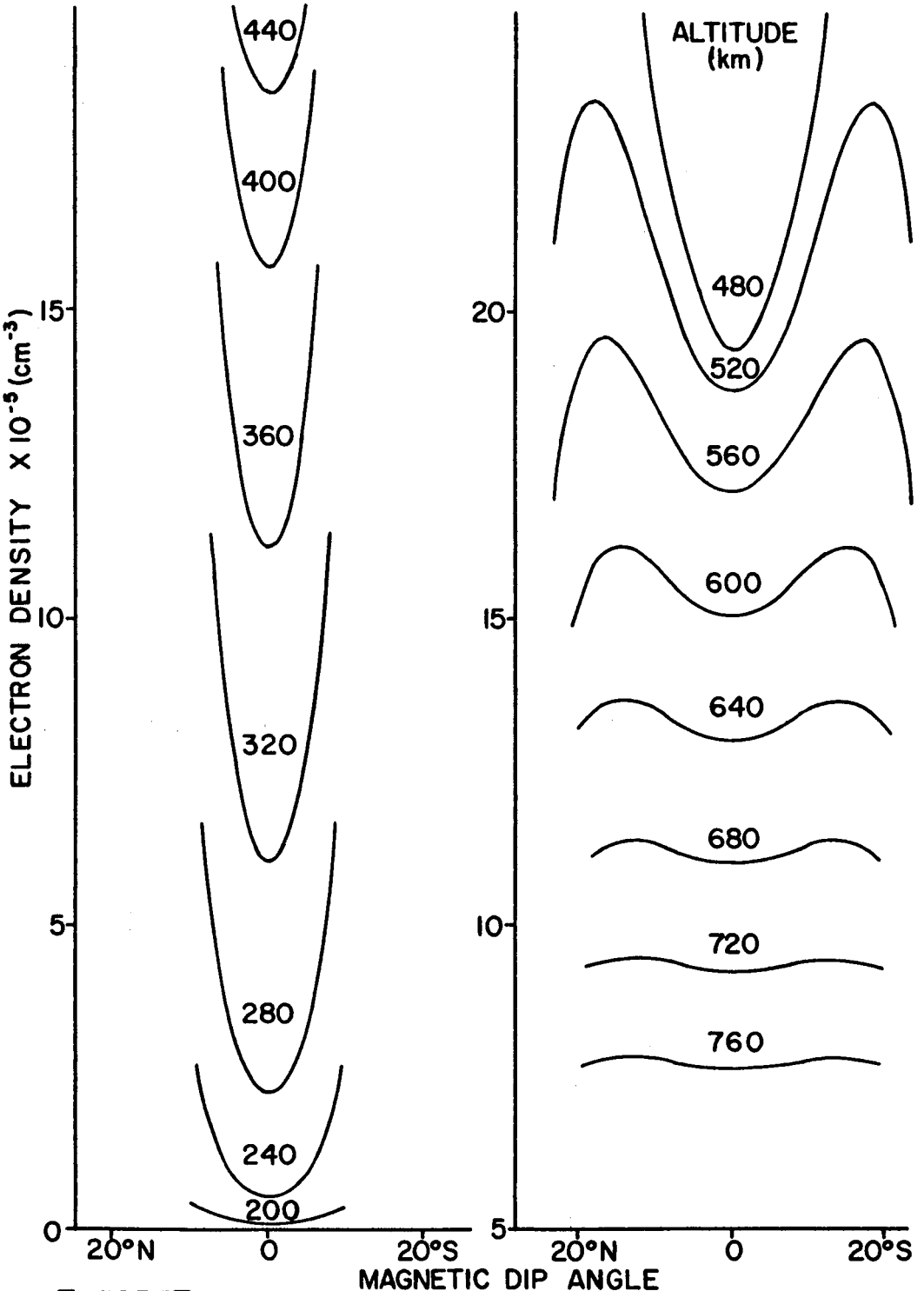

THEORETICAL CURVES OF ELECTRON DENSITY, N, VS. MAGNETIC DIP ANGLE, I, INCLUDING f_4 CASE I: HIGH SUNSPOT NUMBER.

FIGURE 4

and less than this respectively. This figure is in contrast to the 5 per cent increase in "N maximum" as calculated by Kendall, Rishbeth, Lyon and Peart.

Hence the theory developed by Goldberg and Schmerling with the use of a Chapman boundary condition results in a more realistic description of the geomagnetic anomaly.

At a later date Goldberg, Kendall and Schmerling (1964) developed the theory further. Significant changes evolved from the first form of the theory.

In the series solution described previously the difference between production and loss was set equal to zero in evaluating the coefficients in the series solution. This approximation improves with increasing height above the F2 electron peak. The diffusion term then becomes the dominant term and the continuity equation becomes

$$(23) \quad \text{div}\,(N\underline{v}) = 0$$

Using equation (23) and the assumption of diffusive equilibrium along a field line a closed form solution was derived. For diffusive equilibrium along a field line the mean velocity of ions and electrons was set equal to zero. This will be clarified in a later article by Chandra and Goldberg. The equations of

motion of ions and electrons moving along a line of force subject to the Lorentz and gravitational forces and partial pressures were solved. The resulting equation derived along a field line was

$$(24)\quad \frac{1}{N}\frac{dN}{dr} + \frac{1}{2H} = 0$$

This equation was then integrated along a field line and the Chapman boundary condition was invoked. This resulted in the equation

$$(25)\quad N(r,\emptyset) = N(r_o,o)\exp \tfrac{1}{2}\left[1 + k\, r_p - (k\sec^2\emptyset - \frac{\tan^2\emptyset}{H_2})\, r - \exp(kr_p - kr\sec^2\emptyset)\right]$$

where H_2 is the scale height of the ionizable constituent, r_p is the height of the maximum electron density at $\emptyset = 0$. A series expansion of equation (25) subject to the condition

$$(26)\quad kr \gg 1$$

yielded the identical results as Goldberg and Schmerling's earlier theory.

In equation (25) the latitude dependence of $N(r,\emptyset)$ for a fixed height is contained in the third and fourth terms of the exponent. The field line passing through the angular maxima was obtained by maximizing equation (25). This resulted in

$$(27)\quad r_o = r_p - (1/k)\ln(1-1/kH_2)$$

where r_o is the value of r of this field line at

$\phi = 0$. From this equation it is seen that $k H_2 > 1$ is necessary for an angular maximum to occur. Equation (27) was checked favorably with topside sounder information where the angular peaks at constant heights fell on the calculated field line. Applying the extremum condition for a maximum r at constant latitude resulted in

$$(28) \quad r_m = \left[r_p - \frac{1}{k} \ln \left(1 - \frac{\sin^2 \phi}{k H_2} \right) \right] \cos^2 \phi$$

Equation (28) was placed into (25) to find "N maximum" increased steadily to $\phi = 90$ degrees.

The two important points brought out by this extension to the theory are

1) The electron density can have angular maxima at fixed heights only if $kH_2 > 1$

2) No angular maximum occurs in the peak electron density, "N maximum"

Chandra and Goldberg (1964) refined the theory and also examined some of the underlying assumptions made in the derivations of the diffusion term by some authors.

In this work the equations of motion are once again solved with some simplifications made. The assumptions made were the same as listed under Kendall's and Lyon's derivation of the diffusion

term with the exception of the velocity components along a line of force. In Kendall and Lyon's derivations the component of velocity along a field line was assumed greater than the component perpendicular to a field line. The resulting equation which Chandra and Goldberg derived was

$$(29)\quad \frac{M_e b_{en}}{2}\ \underline{V_e}\cdot\underline{h} + \frac{M_i}{4}\, b_{in}\, \underline{V_i}\cdot\underline{h} = -kT\left(\frac{1}{N}\,\text{grad}\, N + \frac{\hat{r}}{2H_2}\right)\cdot\underline{h}$$

where M_e, M_i - mass of electrons and ions

b_{en}, b_{in} collision frequency between electrons and neutrals, and ions and neutrals respectively.

$\underline{h}$-unit vector in direction of magnetic field.

$\underline{h} = -(\hat{r}\sin I + \hat{\phi}\cos I)$

$\hat{\phi}$-unit vector in ϕ direction

$\hat{r}$-unit vector in r direction.

The condition for ambipolar diffusion in a neutral plasma is

$$(30)\quad V_e = V_i = V$$

The condition for diffusive equilibrium is

$$(31)\quad V = 0$$

Chandra and Goldberg point out the assumption the collision frequencies between electrons and neutrals, and ions and neutrals be sufficiently small so that drag forces due to collision be small compared to

gravity, pressure gradients and Lorentz Forces is a more physical restriction in the upper F region than demanding equation (31). In this manner the equation of constraint along a field line was derived from equation (29) when the dipole field relation was used.

$$(32)\quad \frac{1}{N}\frac{dN}{dr} + \frac{1}{2H_i} = 0$$

This is the identical equation to (24)

Although the assumption on the collision frequencies may be more realistic, implicit difficulties result which prohibit explicit solution of the ion and electron velocities from the equations of motion. Difficulty arises in that the electric field between ions and electrons is not known. Hence this prohibits calculations of the velocity components along a field line.

Kendall and Lyon assumed that the velocity parallel to the field lines was much greater than the component perpendicular to the field line. Chandra and Goldberg point out that this does not hold true for all latitudes and the resulting diffusion operator may not be valid in view of this.

Integration of equation (32) was carried out along a field line and a Chapman like boundary

condition with a variable scale height was used. This Chapman profile with a variable scale height was derived by Chandra (1963). The result with this boundary condition is

$$(33)\quad N(r,\phi) = N_p \exp \tfrac{1}{2}\left[1 - \left(\frac{r\sec^2\phi - r_p}{H}\right) + r\frac{\tan^2\phi}{H_i} - \exp\left(-\frac{(r\sec^2\phi - r_p)}{H}\right)\right]$$

where r_p = height of the peak of electron density at $\phi = 0$

N_p = value of the peak electron density at $\phi = 0$.

$$(34)\quad H = H_o\left[1 - a\exp\left(-\frac{a(r\sec^2\phi - r_p)}{2H_o}\right)\right]$$

a = shape factor

$$(35)\quad a = (H_o - H_{op})/H_o$$

H_o = scale height of the ionic constituent

H_{op} = value of H_o at r_p

Values of a from 0.1 to 0.4 represent reasonable values corresponding to normal ionospheric conditions.

Curves for $N(r,\phi)/N_p$ vs latitude were plotted for constant heights and variations of a.

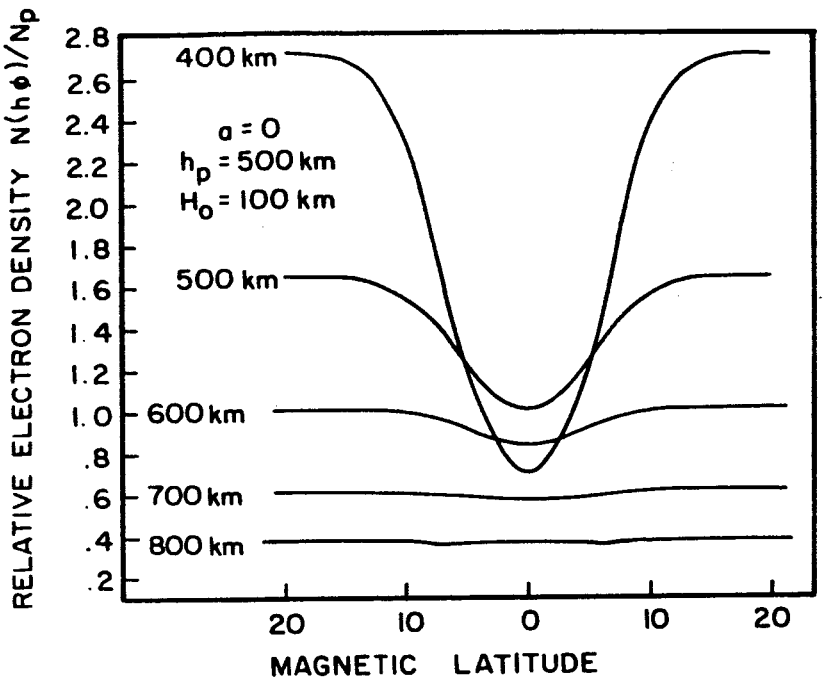

CONSTANT HEIGHT PROFILES OF RELATIVE ELECTRON DENSITY VERSUS LATITUDE FOR $a = 0$, $h_p = 500$ km, $H_o = 100$ km.

FIGURE 5

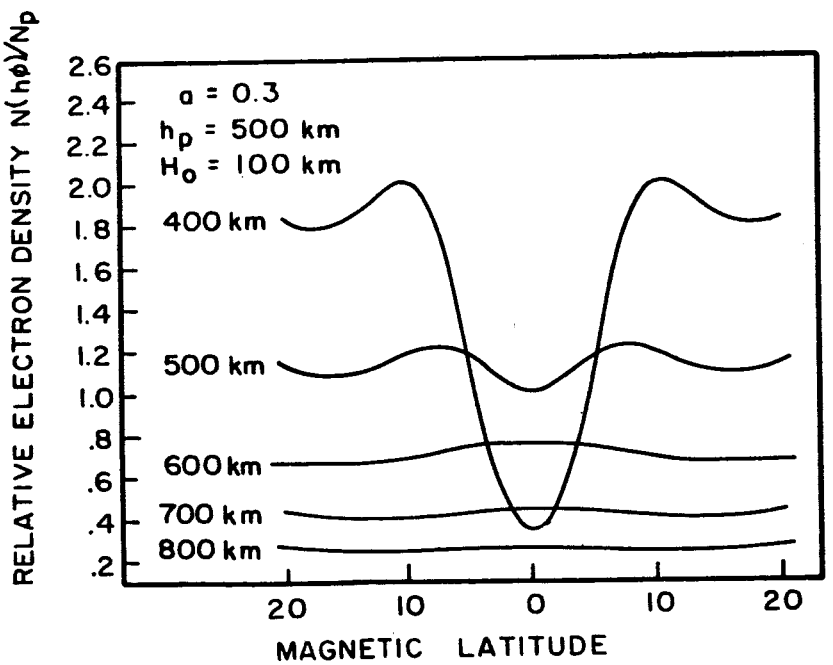

CONSTANT HEIGHT PROFILES OF RELATIVE ELECTRON DENSITY VERSUS LATITUDE FOR $a = 0.3$, $h_p = 500$ km, $H_o = 100$ km.

FIGURE 6

These showed N at a constant height increasing with latitude. The peaks occurring at roughly ten degrees became more resolved with values of "a" from 0.1 to 0.4. Examples of the curves obtained are illustrated in Figures 5 and 6.

The important points to be noted from Chandra and Goldberg's work are:

1) The equation of constraint and the physical assumption concerning the collision frequencies in deriving equation (32).

2) The form of the Chapman like boundary condition with a variable scale height.

In a preprint Goldberg (1964) studies the effect of a variable electron temperature and the effects of a variable acceleration of gravity on the equatorial anomaly. The three important features are

a) The effect of a variable acceleration is sufficient to resolve the angular peaks at constant heights.

b) The effect of a variable electron temperature with height adds another term to the equation of constraint.

$$(36)\quad \frac{dT}{T} + \frac{dN}{N} + \frac{dr}{2H_t} = 0$$

where

$$(37)\quad H_t = \frac{kT}{M_i g}$$

$$(38)\quad T = \frac{T_e + T_i}{2}$$

c) The theory can be extended to the bottomside two scale hits below "N maximum".

A variable electron temperature modified the features of the geomagnetic anomaly slightly.

D. Summary

We have seen in this chapter development of the diffusion theory concerning the equatorial anomaly. Earlier works of Kendall and Lyon's development of the diffusion operator are subject to some criticism in view of Chandra and Goldberg's work. The incorporating of a Chapman boundary condition into the problem has led to a realistic description of the geomagnetic anomaly but the underlying description of the diffusion processes has been sacrificed.

It must be the future goal to replace the assumed boundary condition by one derived from fundamental considerations. This is handicapped by the unknown electric field between electrons and ions in the ionosphere in the equations of motion.

Two main viewpoints were discussed in this chapter. First Kendall, Rishbeth, Lyon and Peart start with the diffusion operator, assume explicit forms for production and loss, specify general boundary conditions and numerically integrate the equilibrium continuity equation. Goldberg et al. derive an equation of constraint assuming diffusive equilibrium along a field line, specify a Chapman boundary condition and obtain a closed form solution. This procedure at the present time gives results which agree more closely with actual ionosphere. The theory is believed to be valid for the topside ionosphere and to be applicable approximately two scale heights below the height of "N maximum". Care must be taken before dismissing the earlier approach. Apparently the general boundary condition leads to difficulties. Also corrections must be made to Kendall et al. approach. It is possible that with refinements to their approach satisfactory results may be obtained. One should not dismiss the earlier work on the results they give. Some inference to this will be given in Chapter Five in view of a recent publication.

CHAPTER III - METHODS OF INVESTIGATION

Basically there are three separate calculations available that will illustrate whether the work of Goldberg et al. provides a reasonable working model of the equatorial anomaly. These concern: 1) the equation of constraint along a field line equation (32), 2) the choice of a Chapman like boundary condition and 3) the predicted variation of total electron content with latitude from the proposed model of Chandra and Goldberg.

A. Equation of Constraint

To show that the equation of constraint leads to a reasonable description of the electron density distribution along a field line when the geomagnetic anomaly exists, the scale height of the ionizable constituent is solved for from the equation. This gives from equation (32)

$$(39) \quad H_i = -\frac{N}{2} \frac{1}{\frac{dN}{dr}}$$

The rate of change of N with r along a magnetic field line was computed from published topside profile data obtained from the Alouette satellite near Singapore. These data consist of values of electron density at 10 kilometer height intervals below the satellite, and are tabulated at

approximately one degree intervals along the satellite orbit, which lay closely along a meridian of longitude. Each profile was computed independently by the personnel of the Radio Research Station, Slough, England. An eccentric dipole model for the earth's magnetic field was used to calculate the geometry of different field lines through these data, and plots were made of N as a function of latitude $\emptyset$ along the various field lines. Considerable scatter was found in the data, especially near the equator, where r changes slowly with latitude and therefore where scaling errors are most important, but more systematic behavior was found further from the equator where the inclination of the field lines is greater. Values of $\frac{dN}{dr}$ evaluated between latitudes 2° and 6° were used to calculate scale heights using equation (39), and these results are tabulated in Section IV of this study.

B. Total Electron Content Methods

In order to investigate the effectiveness of the theoretical predictions in predicting electron content, both at the equator and as a function of latitude, use is made of data collected at Huancayo, Peru, using the Faraday effect in the 54 Mc/sec

beacon transmissions of the Transit 4A satellite. The high frequency or first order theory of the Faraday effect shows that the plane of polarization or a radio wave passing through the ionosphere is rotated by an angle

$$(40)\quad \Omega_o = \frac{\pi e^3}{\lambda m^2 w^3} \int B_L \sec \phi \, Ndh$$

$$(41)\quad = \frac{e^3 \overline{B_L \sec \phi}}{\epsilon_o 8\pi^2 c m^2 f^2} \int Ndh \quad \text{radians}$$

where

ϕ - zenith angle

c - velocity of light

m - mass of electron

ϵ_o - permittivity of free space

e - charge of electron

f - wave frequency

$\overline{B_L \sec \phi}$ - weighted value of the component of the magnetic field along the straight line to the receiver

Ω_o - angle of rotation of the electric vector in traversing the ionosphere

From equation (41) the total electron content can be calculated.

$$(42)\quad N_{Tl} = \int Ndh = \frac{3.879 \times 10^{20} \Omega_o}{\overline{B_L \sec \phi}}$$

where a 54 megacycles frequency is used corresponding to Transit 4A. N_{T1} is the first order total electron content in a meter square column to the height of the satellite (approx. 1000 km). The use of this effect in calculating electron content near the magnetic equator is discussed by Blumle (1961).

W. J. Ross (1964) has extended the Faraday effect equations to include second order effects. These concern departures from the straight line propagation on which the first order theory is derived. Considerations of non-uniform distribution of ionization, anisotropic medium and a non-linear refractive index in electron density and magnetic field intensity are taken into account. The second order polarization rotation angle was derived as

$$(43) \quad \Omega = \Omega_o \left[1 + \tfrac{1}{2} B\overline{X} + \tfrac{1}{2}(B-1)\, G\overline{X} \right]$$

where

Ω_o = first order polarization rotation angle given by equation (41)

Ω = second order polarization rotation angle given by equation (41)

$B = \dfrac{\overline{X^2}}{(\overline{X})^2}$ = a measure of the non-uniformity of the ionization distribution over the height

of integration to the satellite.

= 2.5 for a Chapman layer with a scale height of 67 km and the height of the satellite at 1000 km.

$$\overline{X} = \frac{e^2}{\epsilon_o m 4\pi^2 f^2} \quad \frac{\int_o^{h'} Ndh}{h'}$$

h' = height of the satellite

G = A geometrical parameter involving the direction of straight line propagation, magnetic field, and the vertical at the ionospheric point near which the bulk of the ionization lies. The values of G, $\overline{B_L \sec \phi}$ and ionospheric point were calculated for the Huancayo station by the N.A.S.A. Goddard Space Flight Center, Greenbelt, Maryland.

In the computations N_{T1} for different latitudes was used to calculate $\overline{X}$. Computations for the second order electron content were made for long duration satellite passes corresponding to satellite latitudes ranging from about zero degrees to twenty-five degrees south geographic latitude over Huancayo. A revised rotation angle, Ω', corrected for second order effects, was computed and used in equation (42) to compute a second order total content for each satellite latitude.

$$(44)\quad N_{T2} = \frac{3.879 \times 10^{20}}{B_L \sec \phi}\,\Omega'$$

Plots of N_{T2} vs ionospheric latitude were then made and are discussed in Section IV.

The second order correction amounts approximately to a five per cent reduction in the first order result at geographic satellite latitudes of zero and twenty-five degrees for Transit 4A at a frequency of 54 megacycles, during the daytime. The correction is smaller for closer points in the satellite pass, so that this procedure will modify the form of any trough in electron content.

The general tendency of the second order calculations is to decrease the first order electron content at large zenith angles and to give some smoothing to the data. For a range of positions nearly overhead, the quasi-longitudinal propagation assumption made in the first and second order Faraday Rotation theories breaks down. Also near this condition the polarization rotation angle is small and cannot be measured very accurately. Consequently there is often considerable scatter of data points near the transverse propagation condition (magnetic equator) and a detailed study of the variations in electron content at small latitudes is

not possible.

C. Chapman Profile Assumption

The electron content at the magnetic equator, determined from Faraday effect data as outlined above, may be examined to determine whether the measured values are consistent with the model chosen by Chandra and Goldberg. For this purpose, ionograms taken at the Huancayo site at the same times as satellite passes, were reduced to bottomside electron density profiles and were fitted with a Chapman function topside profile. For this purpose a constant scale height model was used with the scale height being determined 50 km above the peak in electron density, using the temperature at that height given by the Harris and Priester (1962) model of the atmosphere at the appropriate time of day and at the value of 10.7 cm solar radio flux corresponding to the measurement. Atomic oxygen was assumed to be the ionizable constituent .

The resulting N-h profiles were then integrated numerically to give the total electron content in a meter squared column at the equator. The comparison of these values with those measured experimentally is made in Section IV.

D. Total Content Variation with Latitude

From the curves of N_{T2} vs latitude a comparison can be made with the predicted variation of N_T with latitude from Chandra and Goldberg's model.

The curves of N_{T2} vs geographic latitude corresponds to a nominal six to eight degree magnetic latitude range on each side of the magnetic equator. Hence it is sufficient to look at the predictions for the total electron content vs magnetic latitude given by equation (33) for $a = 0$. An additional simplification is made that $H_o = H_i$. This assumption is reasonable for the height range used in the calculations. Actually this assumption becomes better at heights above the peak electron density as shown by Chandra (1963). Values of $H_o = 75$ km, and $H_o = 100$ km were chosen to correspond to a typical mid-day value for atomic oxygen. With these assumptions N-h profiles are calculated for magnetic latitudes from zero to eight degrees in one degree increments. The height ranges taken were from 100 km below the peak of electron density to 700 km, and also from the peak to 700 km. The lower bound was taken because in Goldberg's latest article (1964) concerning the effects of a

variable electron temperature with height, agreement is reached with experiment to almost two scale heights below the electron density peak. The upper bound of 700 km was taken since the Chapman like boundary condition is less valid above this height (Chandra - 1963). At this height N is small compared to the N at the peak, and little contribution to the total electron content comes from greater heights. Each of these curves is numerically integrated to give total electron content in a meter square column. Implicit in these calculations is the fact that no consideration of a geomagnetic anomaly exists below the height mentioned above. As will be seen most of the anomaly arises from the concentrations near the peak of the N-h profile. Above and below a lesser order of absolute contribution is expected.

From the integrated profiles a plot of total electron content vs latitude can be made. Hence direct comparison with the second order Faraday Rotation result is possible. Of particular interest are the comparisons of slope, i.e. the rate of change of content with latitude, and the general shape of the curves.

E. Magnetically Disturbed Days

It is of interest to use the results of the second order Faraday Rotation calculations to study the effects of magnetic storms on the total electron content variation with latitude. The pattern of latitudinal variation will be examined for sequences of days including magnetic storms, for possible correlation of the properties of the anomaly with storms.

F. Diurnal Variation of the Anomaly

Inasmuch as the occurrence of the equatorial anomaly is related to diffusive processes which require time to establish the distribution of ionization, the times of day at which the anomaly is evident are of some interest. The theories of the formation of the anomaly are all equilibrium theories, and are probably most nearly applicable to the ionosphere in the middle to late afternoon, at which time changes in the layers are relatively slow. However we may expect to find an anomaly developing before this time and persisting into the evening when changes in the ionosphere preclude an interpretation of the phenomenon through an equilibrium model.

CHAPTER IV - NUMERICAL RESULTS

Table 1 summarizes the results of calculations made with Chandra and Goldberg's equation of constraint (equation (39)). The date and local time listed are for Singapore. Various height intervals are listed appropriate to calculations made along numerous magnetic field lines within these limits. The average of the computed scale heights is listed for each height interval. The number of individual calculations of scale heights used to compute this average is also listed. Neutral atmosphere scale heights for the extremes of these intervals are listed from the Harris and Priester model of the ionosphere.

TABLE I - RESULTS USING THE EQUATION OF CONSTRAINT

Date (time-local)	Height Interval (km)	Computed Average H_i (km)	No. of Data Points	H. & P. model scale heights	
				height(km)	H(km)
11/9/62	700-600	69	6	700	123
(1209)	600-500	56	8	600	84
	500-400	68	6	500	65
				400	57
12/3/62	655-555	75	9	660	108
(1400)	605-505	63	5	560	74
	555-485	66	12	500	63
				480	61
9/10/63	655-555	76	4	660	112
(1314)	555-505	59	5	560	74
	505-455	69	6	500	60
				460	55
9/13/63	630-530	74	4	640	94
(1248)	630-430	64	13	540	71
				440	60
9/15/63	650-550	71	4	660	91
(1234)	550-450	62	12	560	74
	500-450	65	8	500	68
				450	64
9/22/63	650-550	72	16	660	106
(1138)	600-500	71	18	600	84
				560	75
				500	65

Table II lists the results of fitting a Chapman topside to various N-h profiles taken at Huancayo, Peru during satellite passes of Transit 4A. The time listed for each date is eastern standard time. The height of "N maximum", solar flux (in watts per meter^2 cycles per second) and scale height used are listed appropriate for each time and date. The total electron content computed from the profiles is listed as "N_T(N-h)". The total electron content as given by the second order Faraday Rotation computations is listed as N_T (Faraday). A relative per cent error is computed for comparison. Figure 7 shows the relative error in total content in a meter square column for these profiles as compared to the second order Faraday Rotation analyses whose results are believed accurate to better than five per cent. The relative per cent error is plotted vs time of day for possible correlation with time.

TABLE II - CHAPMAN FIT FOR TOPSIDE OF N-h PROFILES

Date	Time (EST)	Ht. of "N max"	Solar flux 10^{-22} $\frac{w}{m^2 c/s}$	Scale height km	N_T(N-h) 10^{17} electron meters^{-2}	N_T (Faraday)	Relative % error
9/15/61	1800	400	135	65.3	2.74	2.80	-2.0
9/17/61	1700	380	124	63.0	2.87	3.67	-21.7
9/19/61	1730	390	101	56.3	2.36	3.15	-25.0
11/4/61	1845	495	82	73.7	3.11	2.25	38.4
12/7/61	1200	340	94	58.1	3.07	3.74	-17.9
2/16/62	1954	490	86	75.1	3.99	1.75	127.9
3/6/62	1515	380	81	53.6	2.82	3.82	-26.1
3/15/62	1345	360	84	55.0	3.34	3.69	-9.5
4/7/62	1930	330	77	41.9	2.41	2.27	6.2
4/9/62	2030	400	78	51.9	1.99	2.13	-6.7
5/31/62	1915	405	104	54.6	1.28	1.30	-0.9
6/1/62	1930	440	91	57.8	1.16	1.08	7.9
7/24/62	1830	410	78	52.8	1.15	1.00	15.0
11/3/62	1915	350	80	46.6	1.86	2.44	-23.7
12/3/62	1215	340	83	62.4	2.90	3.08	-5.6

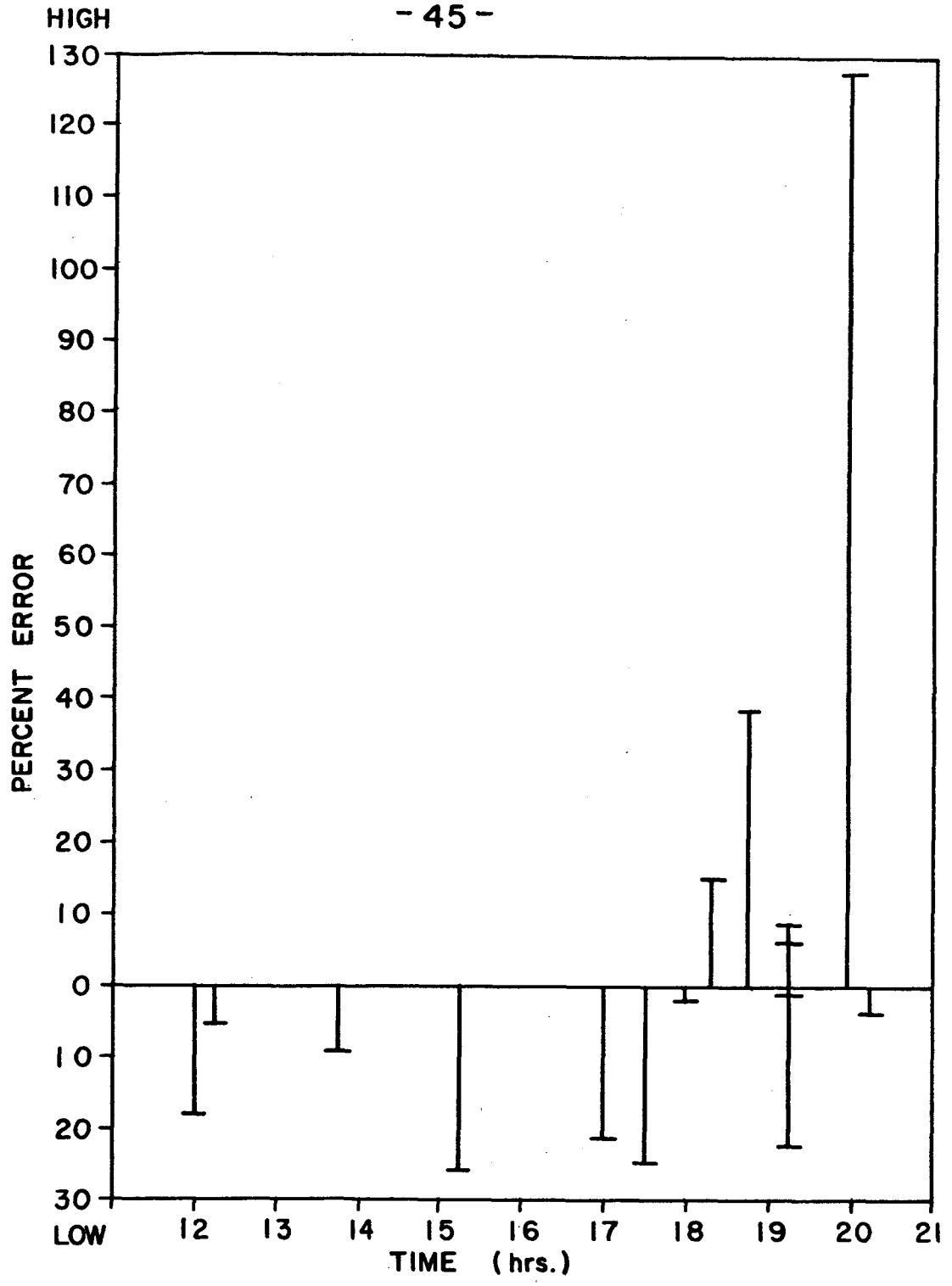

RELATIVE ERROR OF TOTAL ELECTRON CONTENT COMPUTED FROM N-h PROFILES AS COMPARED WITH FARADAY ROTATION RESULTS.

FIGURE 7

Figure 8 illustrates the predicted total electron content vs magnetic latitude for the topside ionosphere based on Chandra and Goldberg's model with a = 0. Figure 9 shows a similar variation with the exception that the total content is calculated from a height 100 km below the peak of the computed N-h profiles. In both figures separate curves appear for scale heights of 75 and 100 km. Table III gives the changes in total content with latitude for the second order Faraday Rotation computations along with the changes predicted by the theoretical model. The notations used in this table are: (_, _) - degrees magnetic latitude used to find changes in total electron content. (_, _)n or s - North and South degrees magnetic latitude.

$\Delta N_T(F)$ - change with latitude of the total electron content as calculated by the second order Faraday Rotation method. A "*" after this value represents the average of $\Delta N_T(F)$ on both sides of the magnetic equator.

ΔN_T(C. & G., H_o = ..., bp or p) - change with latitude of total electron content as predicted by the Chandra and Goldberg model. The value of H_o given in the table specifies the scale height used to calculate the total electron content variation

with latitude for Chandra and Goldberg's model.
"bp" - specifies the total content was calculated from a height 100 km below the height of "N maximum" for each degree of latitude.
"p" - specifies the total content was computed for the topside of the ionosphere only.

Corrections to the theoretical predictions were made to account for a change in "N maximum" for different days.

Figures 10 through 14 illustrate the anomaly in total content. From this type of graph the experimental change in total electron content was determined for Table III. One degree magnetic latitude corresponds to 1.06 degrees geographic latitude.

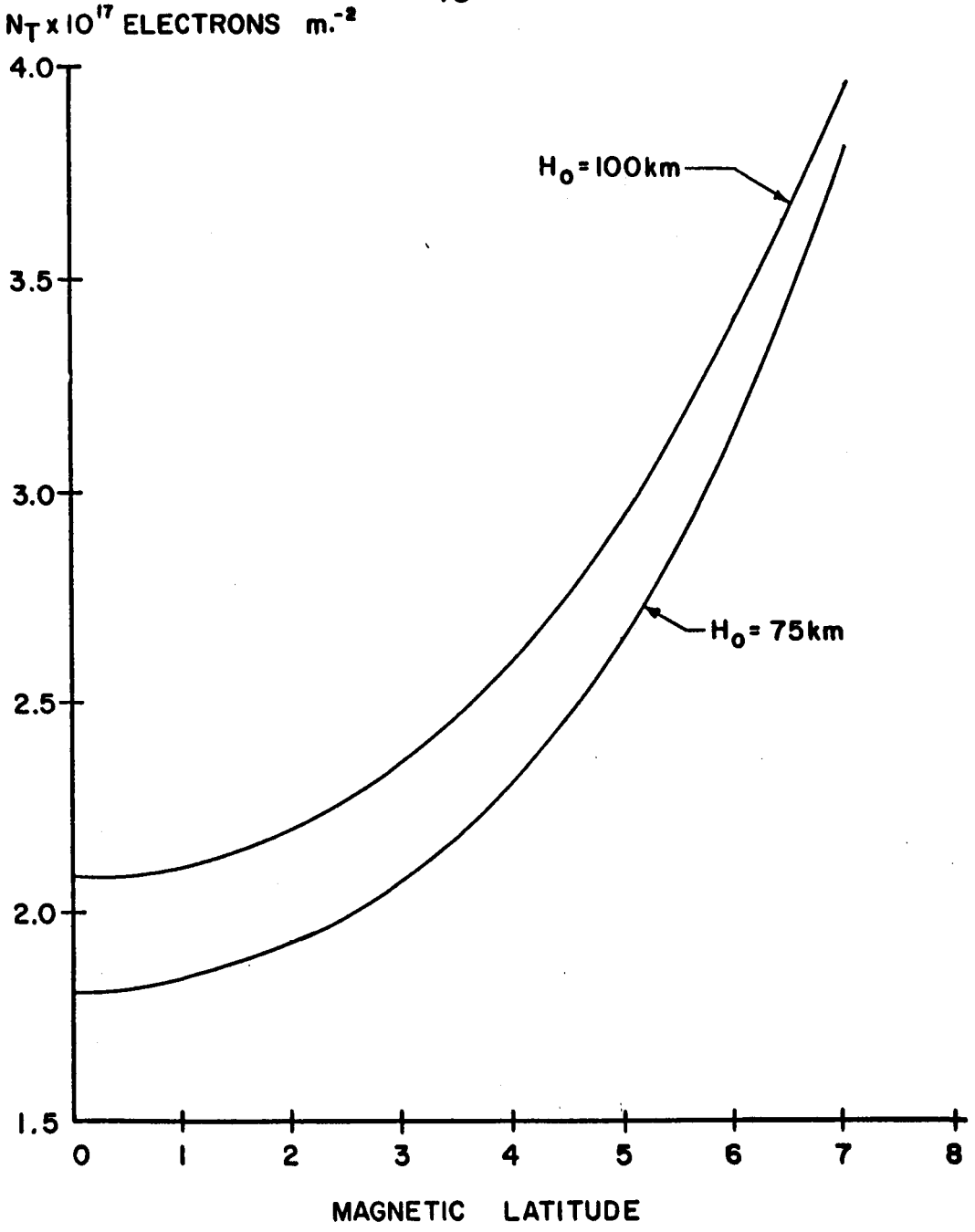

TOTAL ELECTRON CONTENT VARIATION WITH MAGNETIC LATITUDE FOR THE TOPSIDE OF THE IONOSPHERE AS COMPUTED FROM CHANDRA AND GOLDBERG'S MODEL WITH ($\alpha = 0$)

FIGURE 8

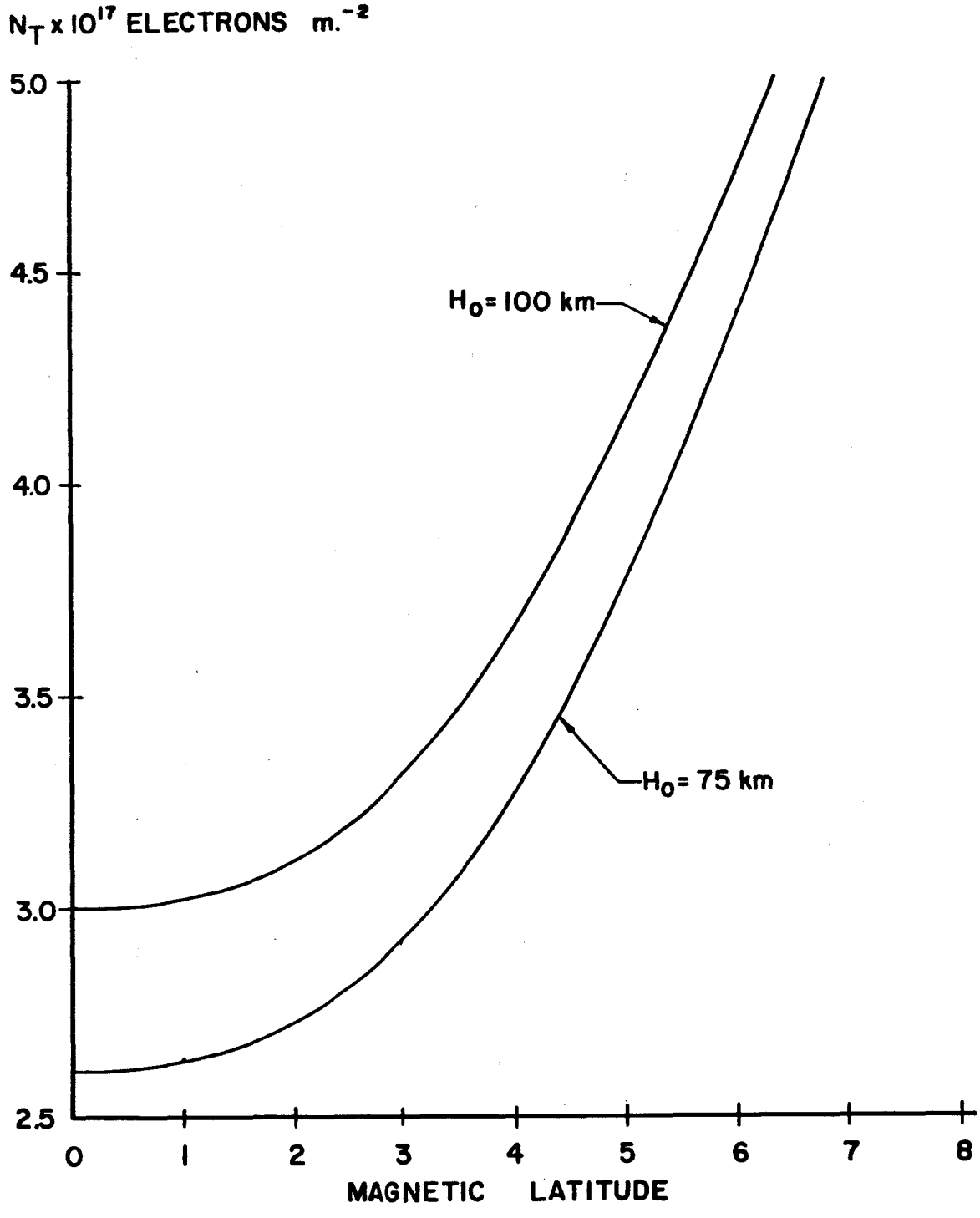

TOTAL ELECTRON CONTENT (COMPUTED 100km. BELOW F_2 PEAK) VARIATION WITH MAGNETIC LATITUDE AS COMPUTED FROM CHANDRA AND GOLDBERG'S MODEL WITH (a=0)

FIGURE 9

TABLE III - COMPARISON OF CHANGE IN TOTAL ELECTRON CONTENT WITH LATITUDE

(1) Date (time) EST	(2) Mag. Lat.	(3) ΔN_T(F)	(4) ΔN_T(C. & G. H_o=75, bp)	(5) ΔN_T(C. & G. H_o=100, bp)	(6) ΔN_T(C. & G. H_o=75, p)	(7) ΔN_T(C. & G. H_o=100, p)
		← 10^{17} electrons/meter^2 →				
9/15/61 (1815)	(2,6)n	0.43*	1.65	1.57	1.17	1.16
	(3,6)s		1.44	1.34	1.06	1.02
9/17/61 (1700)	(2,5)n	0.25*	1.05	1.05	0.70	0.68
	(4,6)s		1.13	1.01	0.85	0.83
9/19/61 (1720)	(1,6)n	0.44*	1.47	1.39	1.05	1.04
	(2,6)s		1.40	1.33	0.99	1.04
11/2/61 (1940)	(1,6)n	0.72	1.51	1.43	1.08	1.07
11/4/61 (1830)	(0,6)n	0.68	1.84	1.74	1.39	1.33
11/5/61 (1845)	(0,4)n	0.65	0.51	0.53	0.38	0.36
11/16/61 (1600)	(2,6)n	0.305*	1.65	1.57	1.17	1.16
	(3,7)s		2.35	2.01	1.70	1.56
12/6/61 (1200)	(1,4)n	0.24	0.74	0.76	0.47	0.49
2/14/62 (1900)	(1,6)n	0.66	1.26	1.19	0.90	0.89
2/16/62 (1930)	(1,5)n	0.42	1.02	1.01	0.68	0.67
3/4/62 (1445)	(1,5)n	0.45	1.59	1.57	1.07	1.04
3/6/62 (1510)	(1,6)n	0.37*	1.74	1.64	1.24	1.23

TABLE III (CONT.)

(1)	(2)	(3)	(4)	(5)	(6)	(7)
	(2,6)s		1.65	1.57	1.17	1.16
3/7/62 (1530)	(1,5)n	0.41	1.56	1.54	1.05	1.02
3/15/62 (1345)	(3,7)n	0.41*	2.80	2.39	2.02	1.85
	(3,6)s		1.72	1.59	1.26	1.21
3/21/62	(1,5)n	0.36	1.24	1.23	0.84	0.82
4/7/62 (1930)	(3,5)n	0.17*	1.10	1.07	0.76	0.70
	(3,5)s		1.10	1.07	0.76	0.70
4/9/62 (1830)	(1,5)n	0.34*	0.97	0.96	0.65	0.63
	(2,7)s		2.23	1.94	1.58	1.48
4/10/62 (1845)	(2,5)n	0.22*	1.22	1.22	0.81	0.79
	(1,5)s		1.33	1.31	0.89	0.87
4/12/62 (1900)	(2,6)n	0.54	1.43	1.36	1.02	1.01
4/19/62 (1720)	(3,6)n	0.29*	1.79	1.66	1.31	1.26
	(1,4)s		0.79	0.81	0.50	0.43
5/31/62 (1915)	(2,5)n	0.29*	0.77	0.77	0.51	0.49
	(2,7)s		1.91	1.67	1.35	1.27
	(2,6)n		0.82	0.78	0.58	0.58
7/24/62 (1830)	(2,7)s	0.29*	1.27	1.11	0.90	0.84
9/18/62 (1820)	(2,5)n	0.30	0.81	0.81	0.54	0.52
9/21/62	(1,3)n	0.29	0.26	0.27	0.16	0.18
11/3/62 (1910)	(0,6)n	0.43*	1.76	1.66	1.33	1.27
	(3,7)s		2.35	2.01	1.70	1.56
12/2/62 (1345)	(2,6)n	0.26	1.43	1.36	1.02	1.01
12/3/62 (1210)	(2,7)n	0.42	2.62	2.29	1.86	1.74

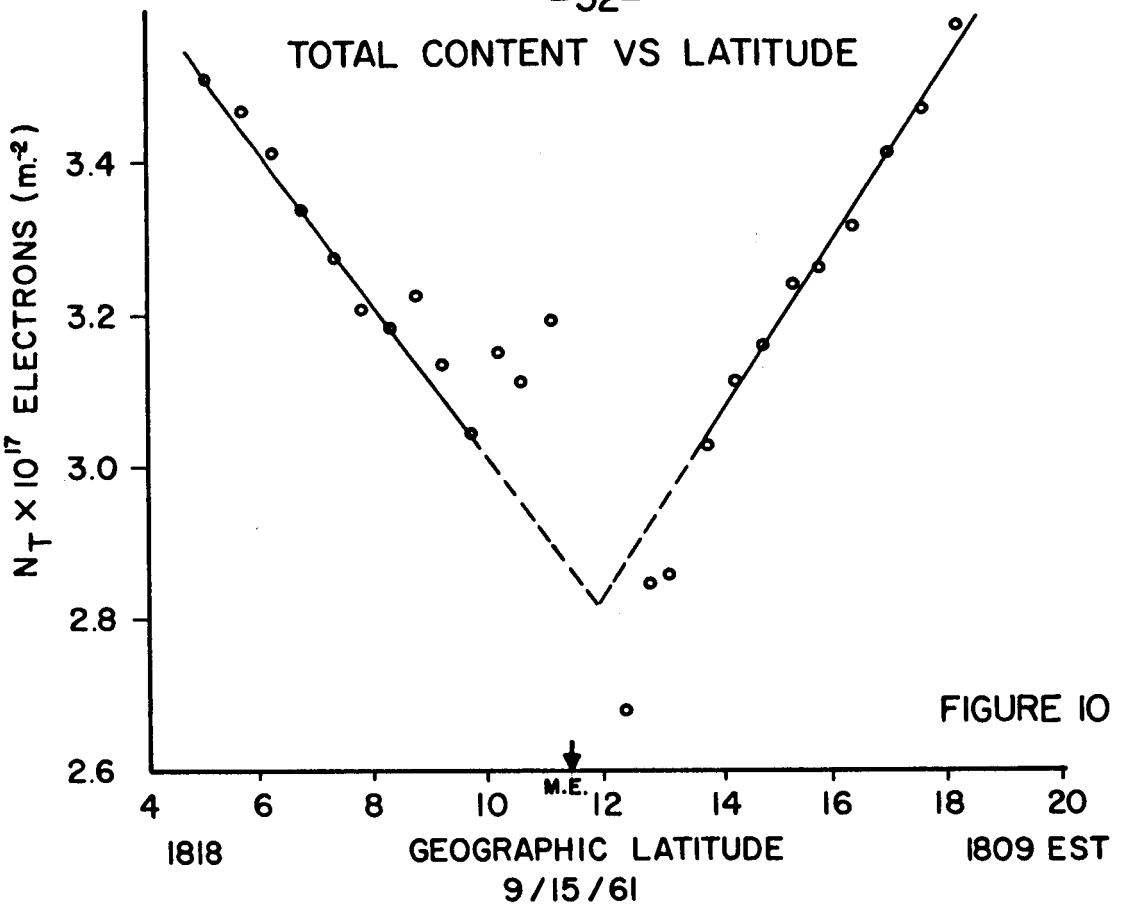

FIGURE 10

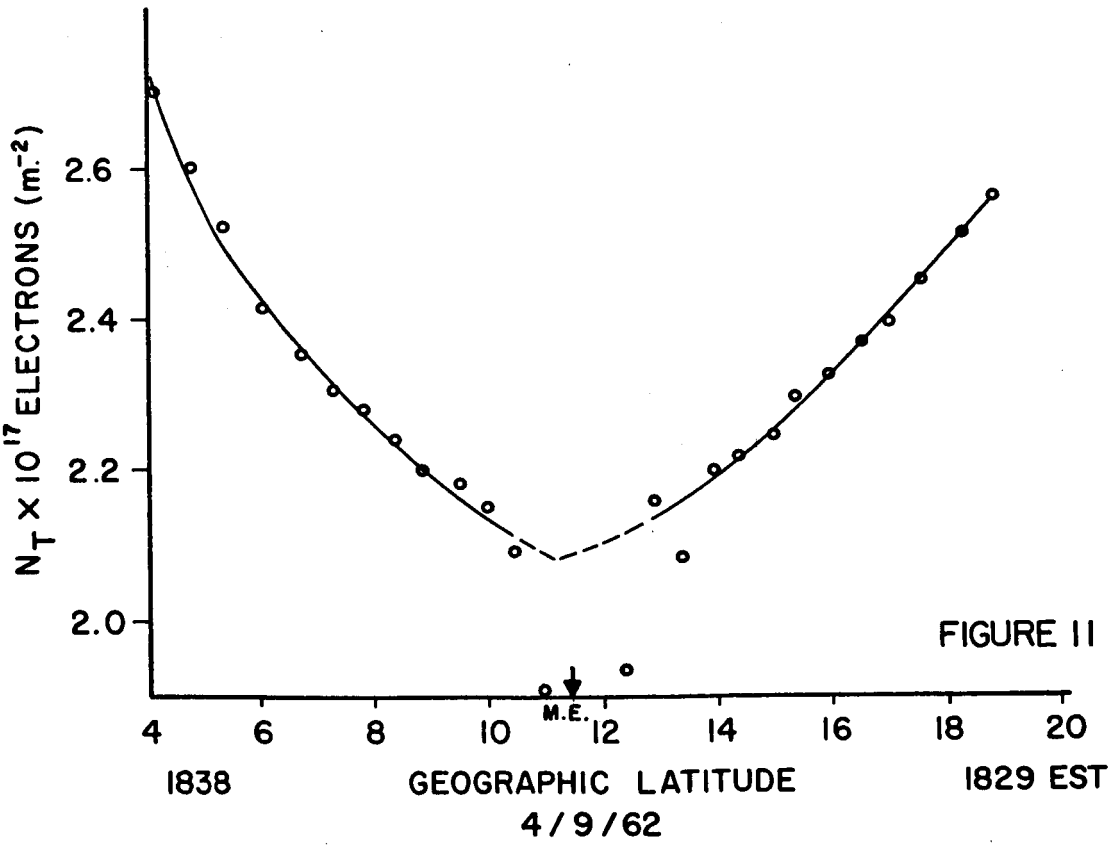

FIGURE 11

TOTAL CONTENT VS LATITUDE

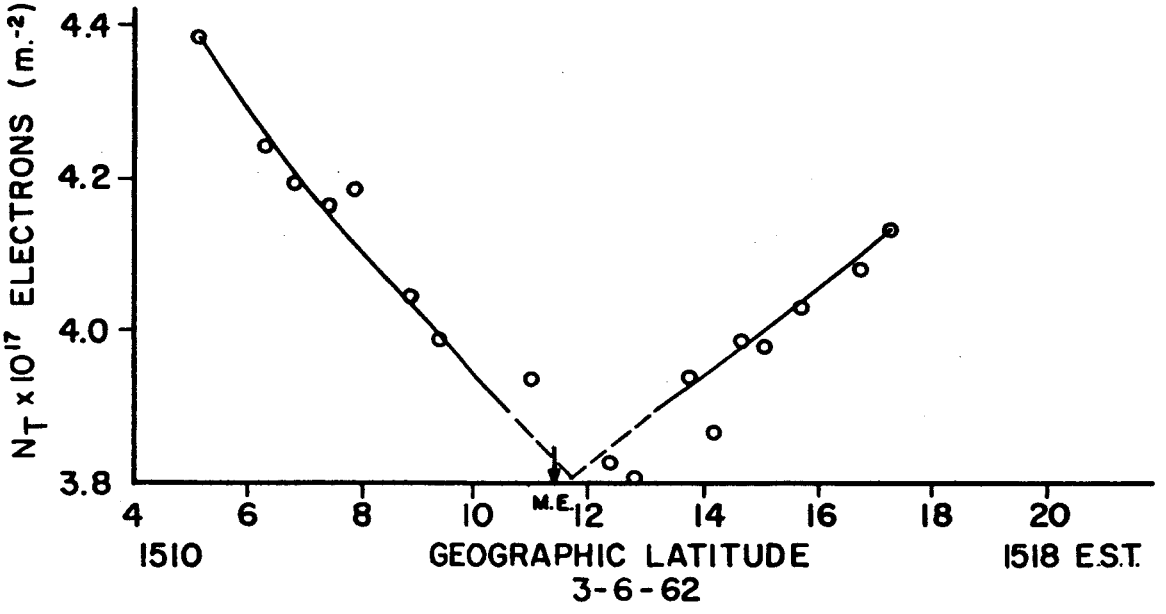

FIGURE 12

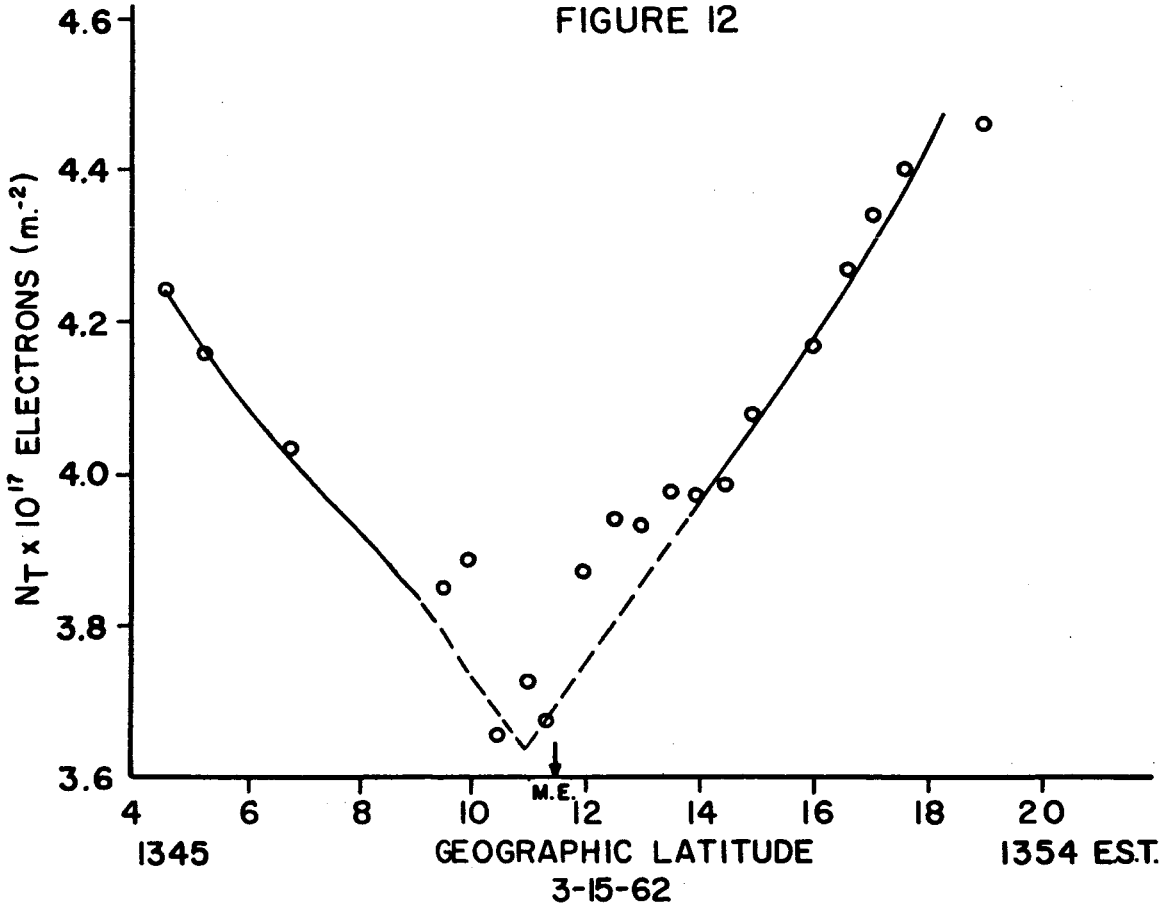

FIGURE 13

TOTAL CONTENT VS LATITUDE

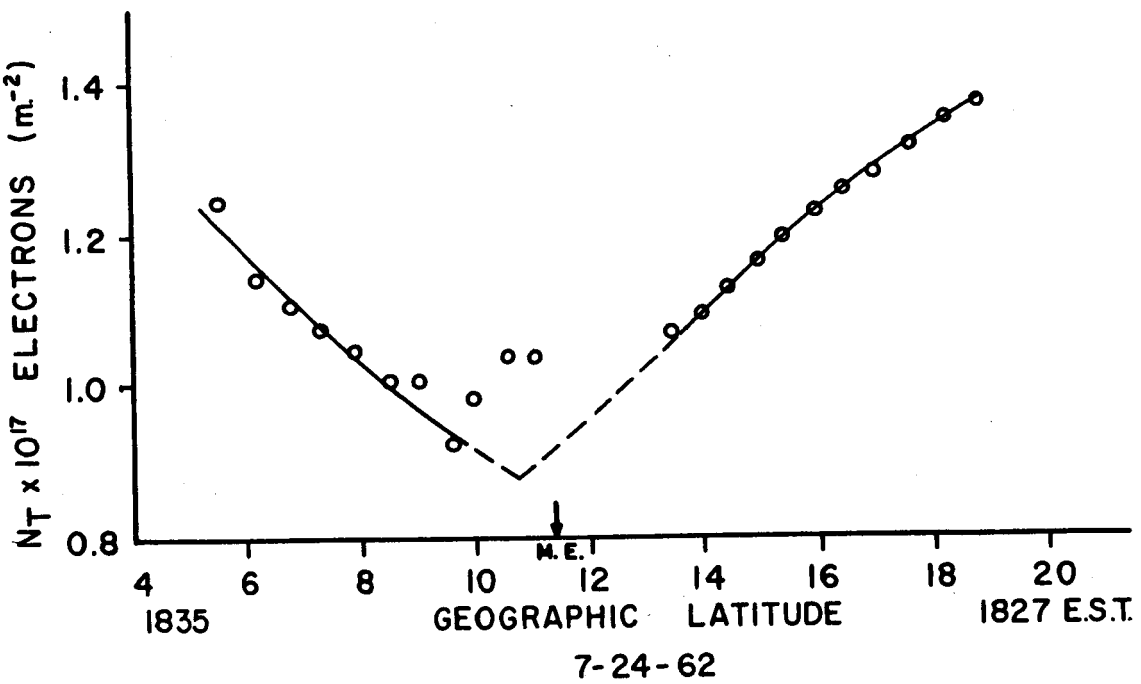

FIGURE 14

Table IV shows an examination of the behavior of the total electron content variation with latitude during periods of local distrubance for Huancayo. A "*" indicates the day on which the storm began, and the time of the onset of the storm is listed. K is a local figure for the intensity of the geomagnetic disturbance. The assigned range of values of K are from 0 (very quiet) to 9 (extremely disturbed). K as great as 5 represents a moderate disturbance while K listed as 6 or 7 represents a moderately severe disturbance. The time for the beginning of the Faraday rotation records is listed along with comments describing the behavior of the total content variation with latitude. The following notations are used under "Comments".

A - Geomagnetic Anomaly is present

N - North side of magnetic equator

S - South side of magnetic equator

? - The geomagnetic anomaly could not be determined from the data for one of the following reasons:

a) Scatter in the data is present

b) There was a lack of a complete record.

c) The increase in total content with latitude was insufficient to indicate clearly the presence of the anomaly.

Figures 15 through 25 illustrate the total content behavior with latitude of three periods listed in Table IV.

NOTE

The geomagnetic anomaly is not present at all times of the day. Figures 26, 27, and 28 illustrate the time behavior of the build up of the geomagnetic anomaly. The sequence of records shown were taken over an interval of 10 weeks and can be interpreted as showing the general time of onset only, rather than the exact time on any particular day.

TABLE IV - STUDY OF MAGNETICALLY DISTURBED PERIODS

(1) Date		(2) Storm begins EST	(3) K	(4) Time of Faraday Rotation Record-EST	(5) Comments
11/4/61				1827	A
5				1842	A
6	*	1818	5	1856	A
8				1738	no A
9				1752	A
11/16/61				1600	A
17	*	0740	6	1616	no A
19				1459	no A
12/5/61	*	0858	5	1459	A
6	*	0640	5	1155	?
7				1211	A
2/14/62				1901	A on N; ? on S
15	*	1020	7	1915	no A
16				1929	A
17				1943	?
18				1826	no A
19				1840	A
3/4/62				1443	A on N, ? on S
5	*	0650	5	1456	? on N, A on S
6	*	0530	6	1510	A

TABLE IV - (CONT.)

(1)	(2)	(3)	(4)	(5)
7 *			1524	A on N, ? on S
4/7/62			1932	A
8			1945	?
9			1829	A
10 *	0500	5	1844	A
12			1857	A on N, ? on S
4/19/62			1720	A
20 *	1856	6	1548	A
21			1602	A
9/18/62*	1931	5	1822	A on N, ? on S
19			1836	?
21			1719	A on N, ? on S
11/29/62*	1945	4	1301	no A
30			1314	no A
12/2/62			1344	A on N, ?S
12/3/62*	2234	6	1711	A
4			1725	no A
5			1741	no A

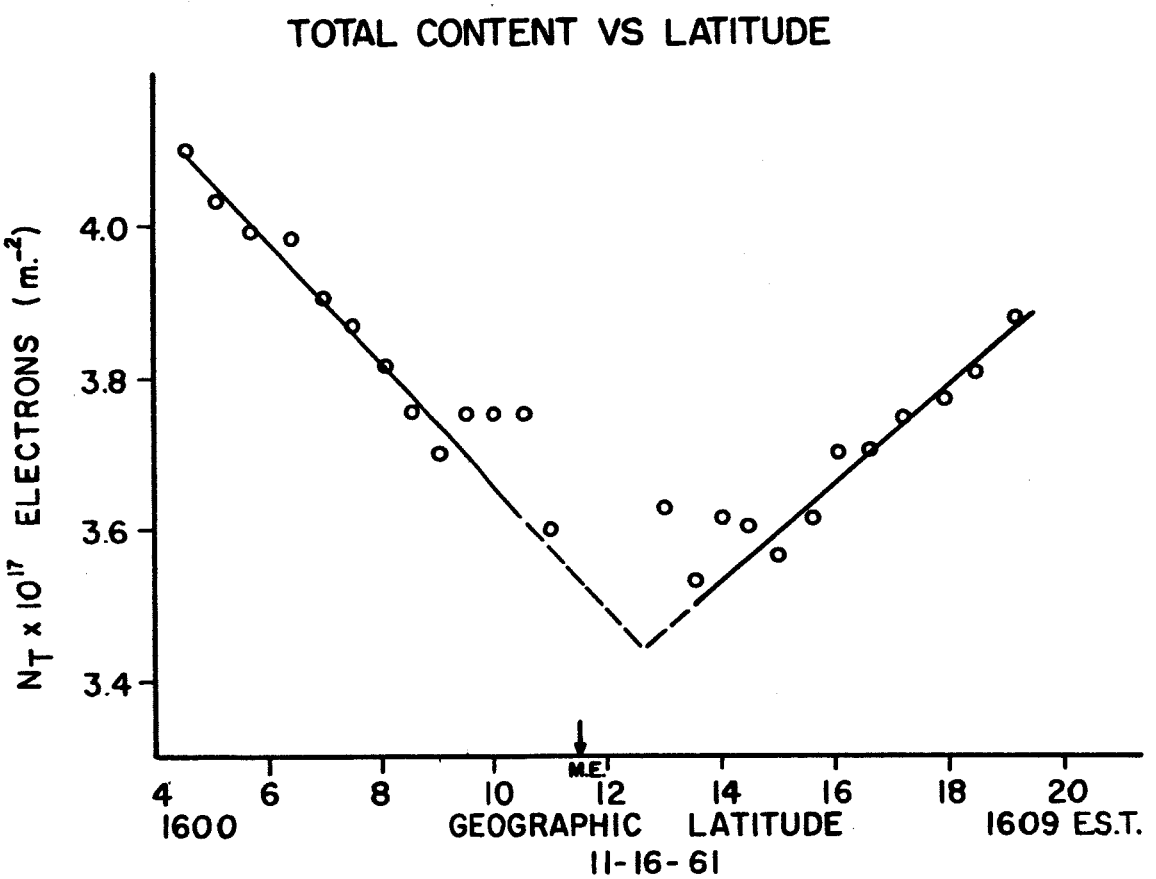

FIGURE 15

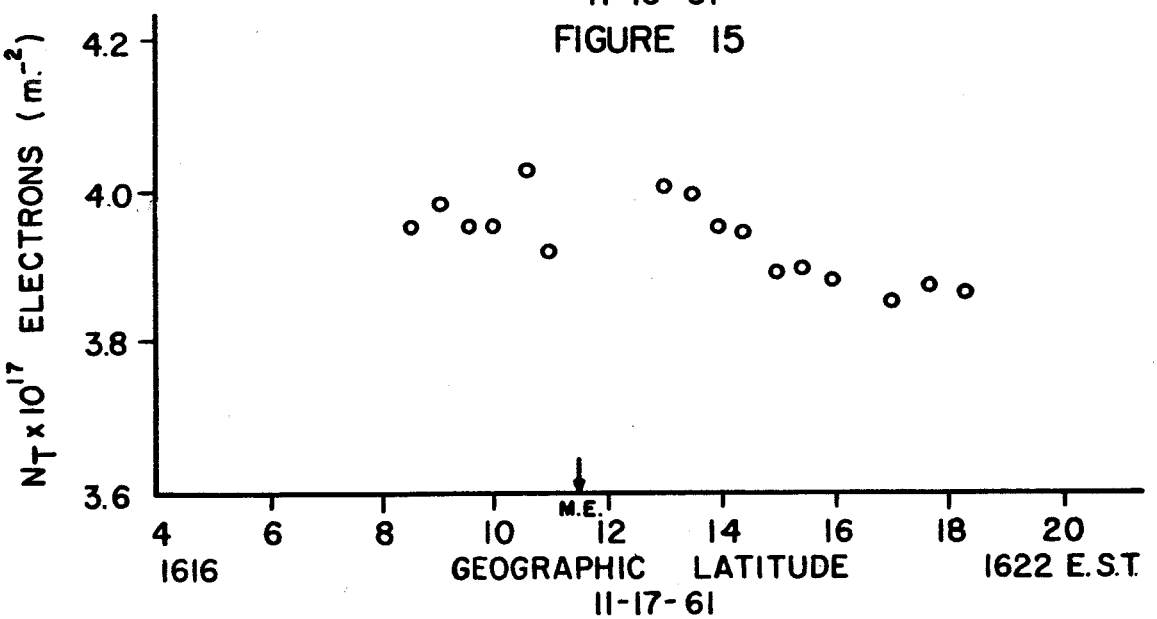

FIGURE 16

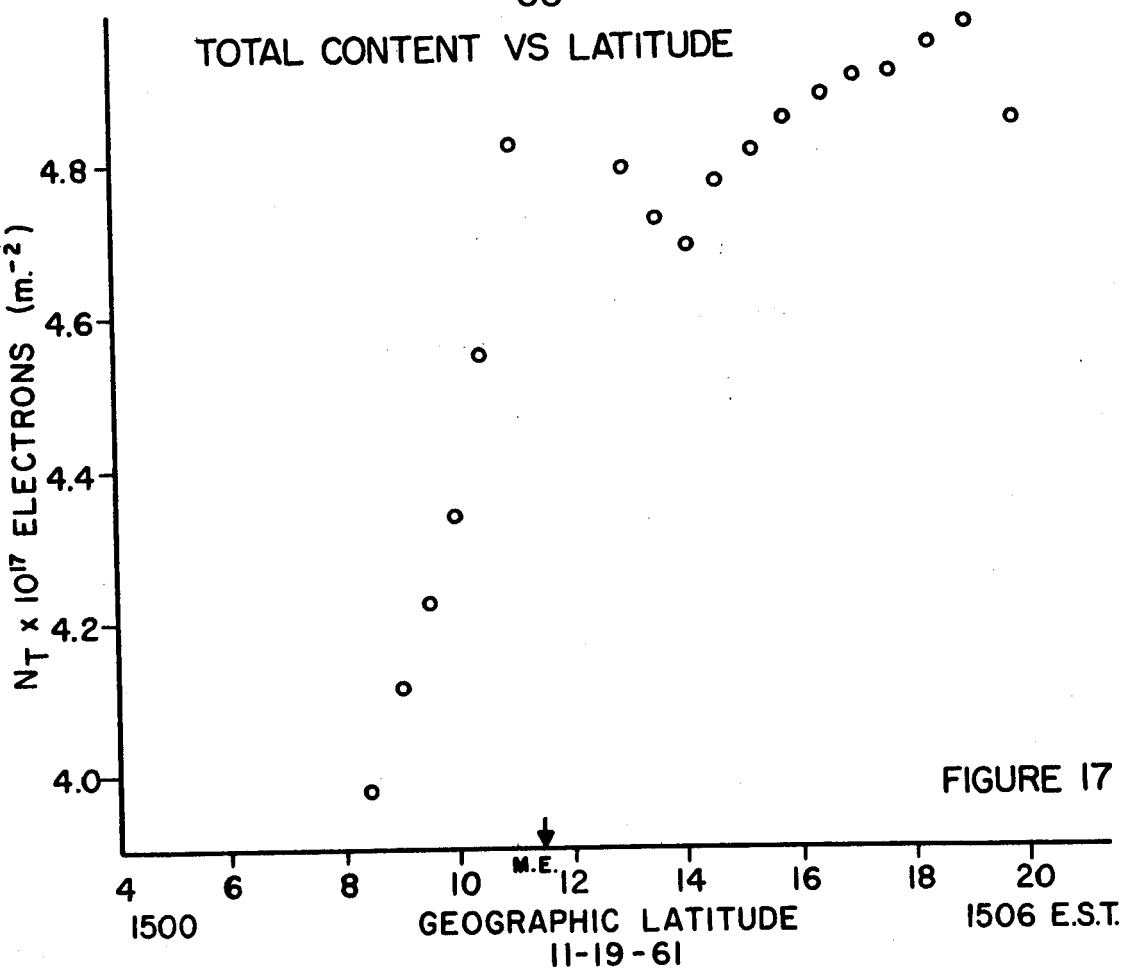

FIGURE 17

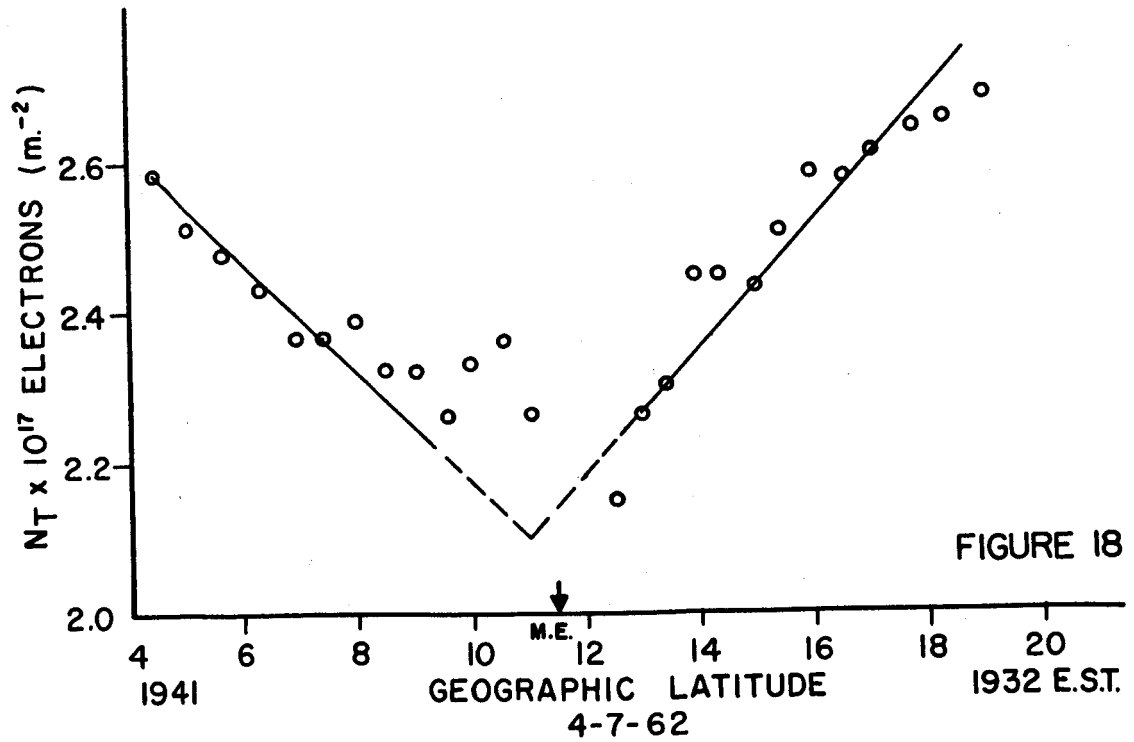

FIGURE 18

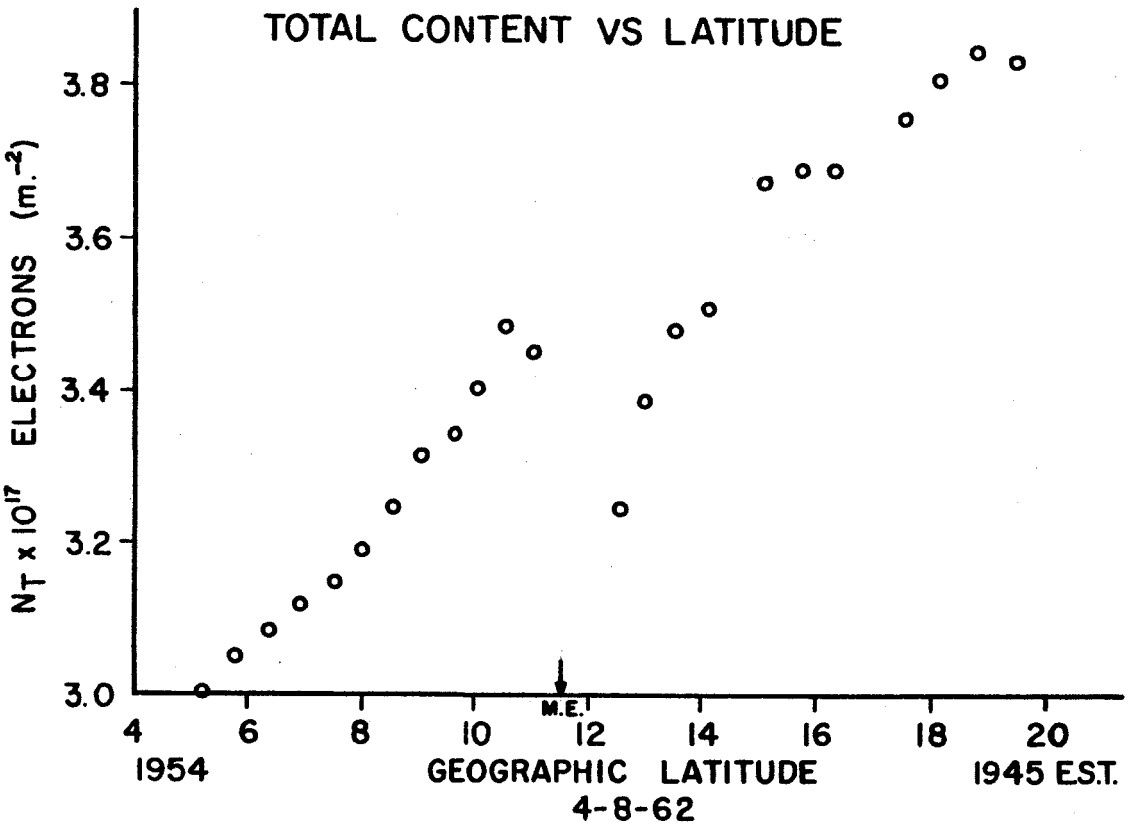

FIGURE 19

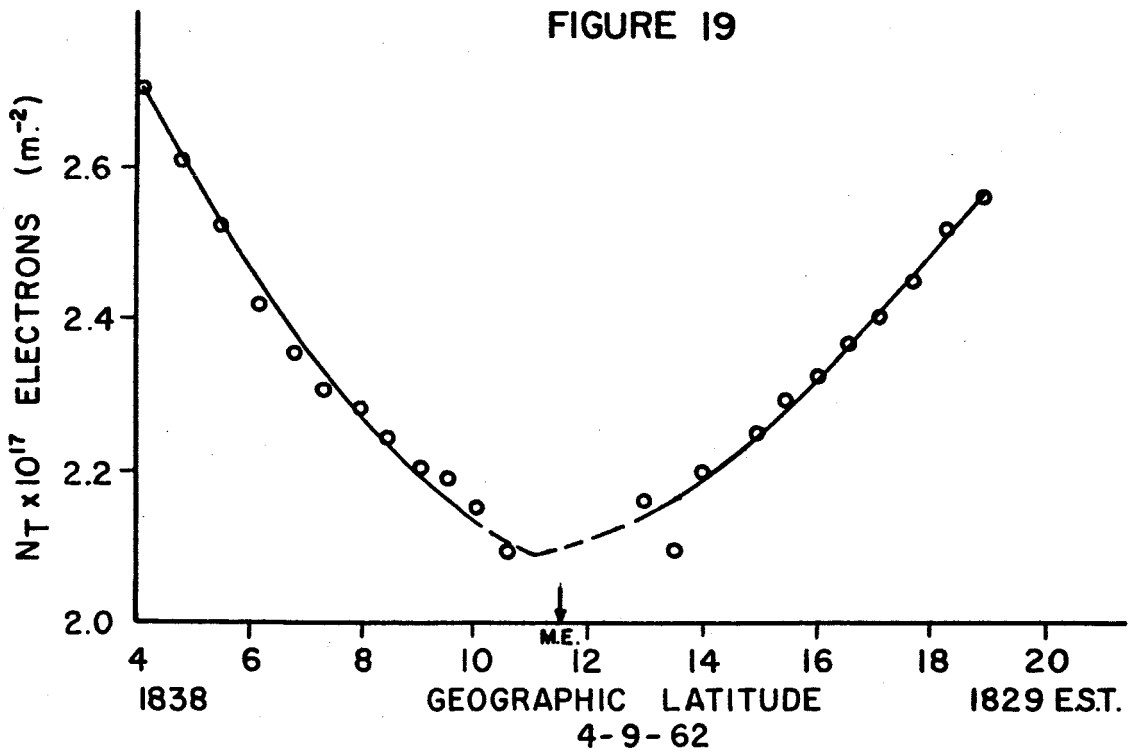

FIGURE 20

TOTAL CONTENT VS LATITUDE

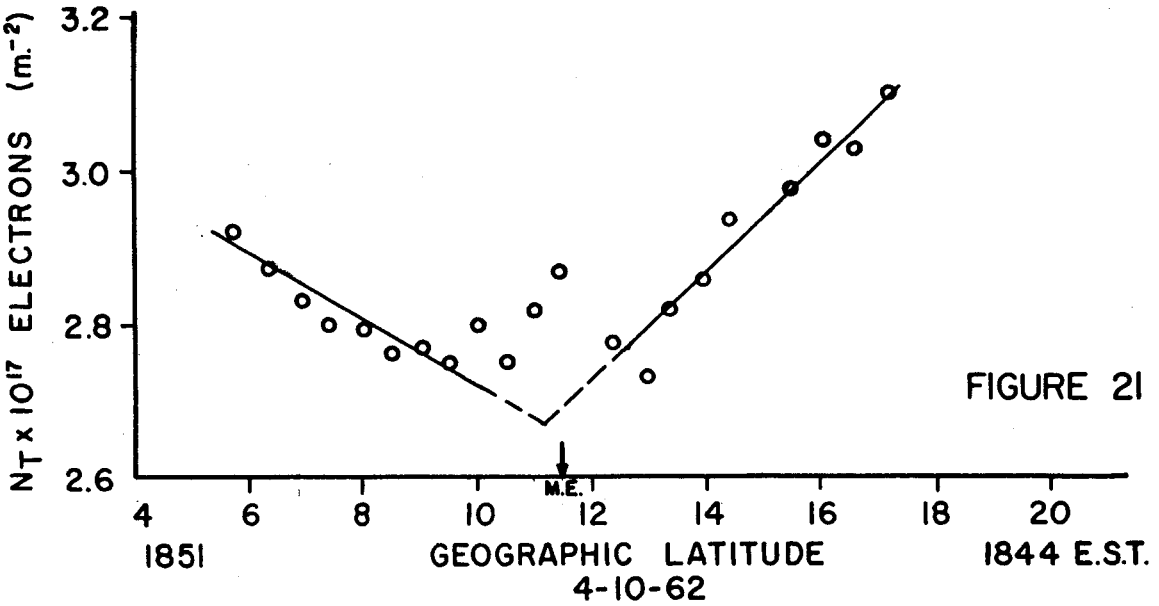

FIGURE 21

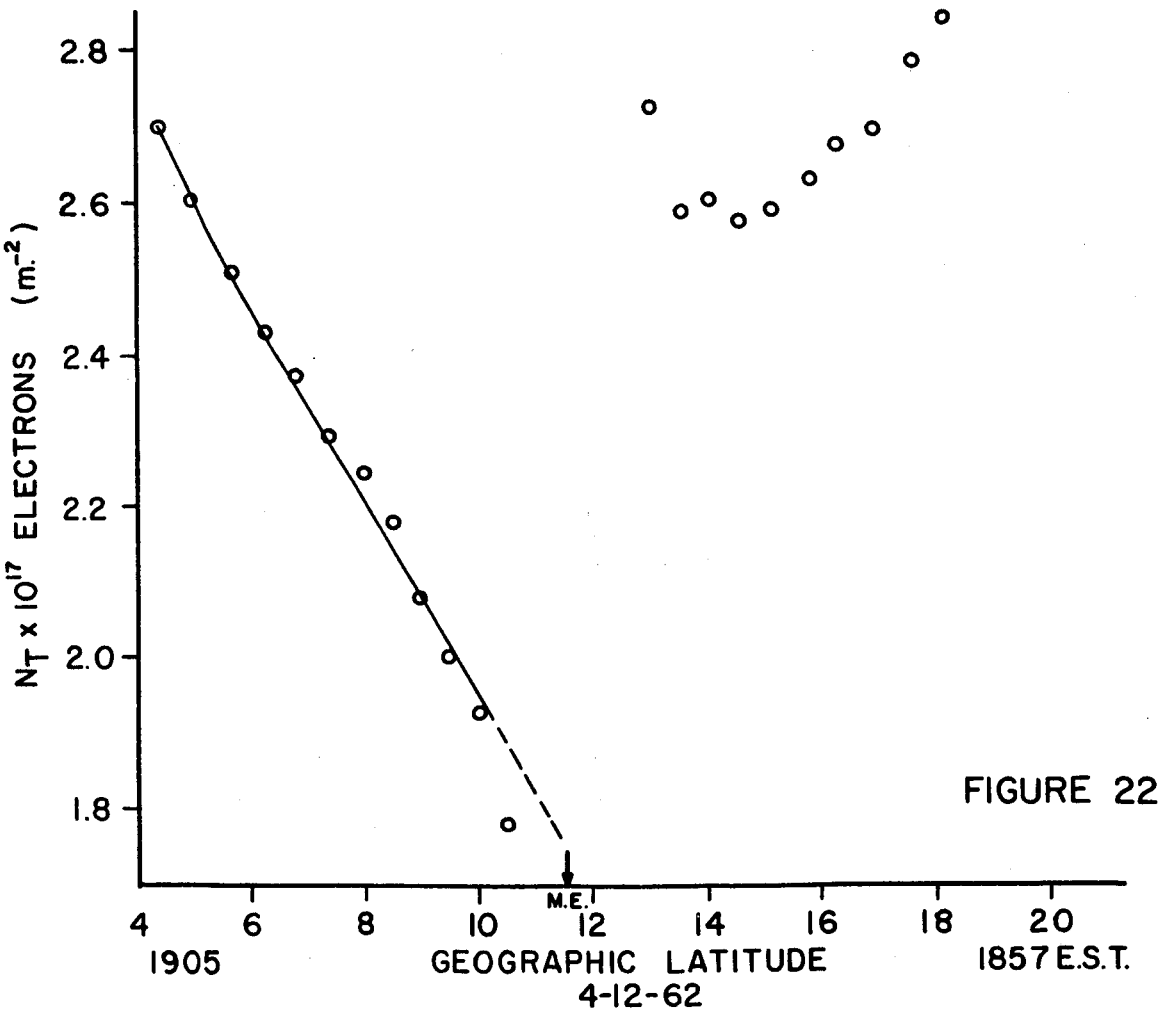

FIGURE 22

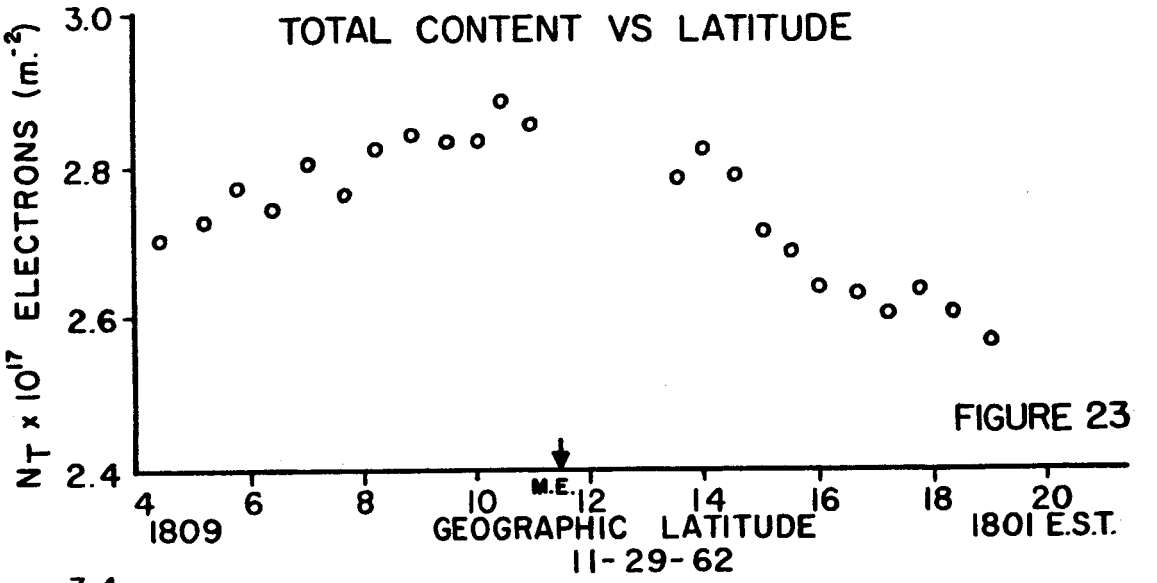

FIGURE 23

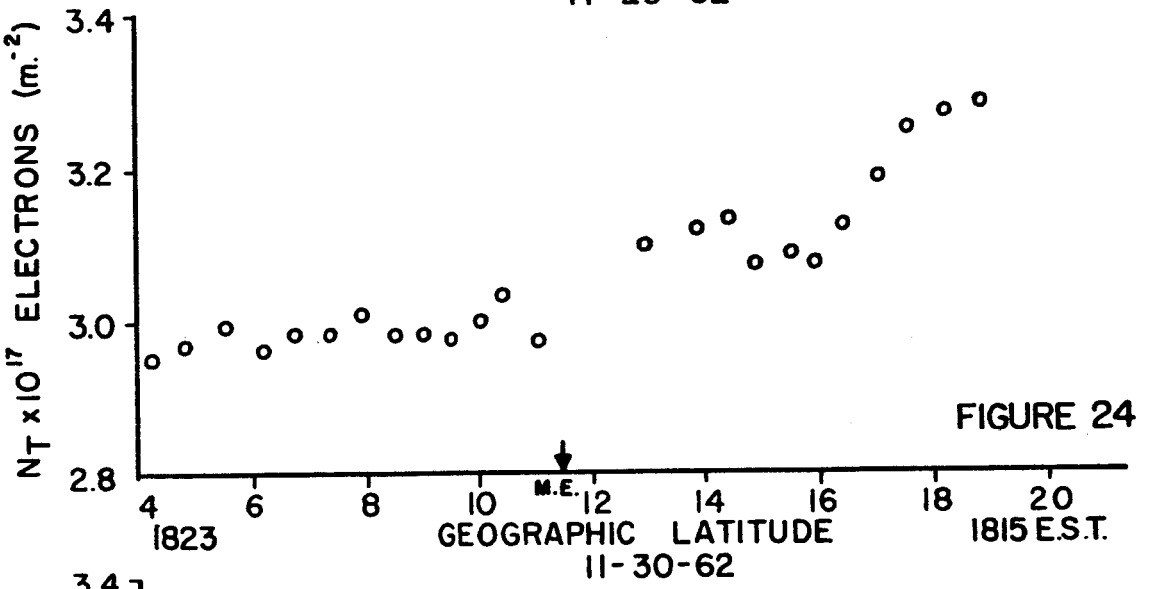

FIGURE 24

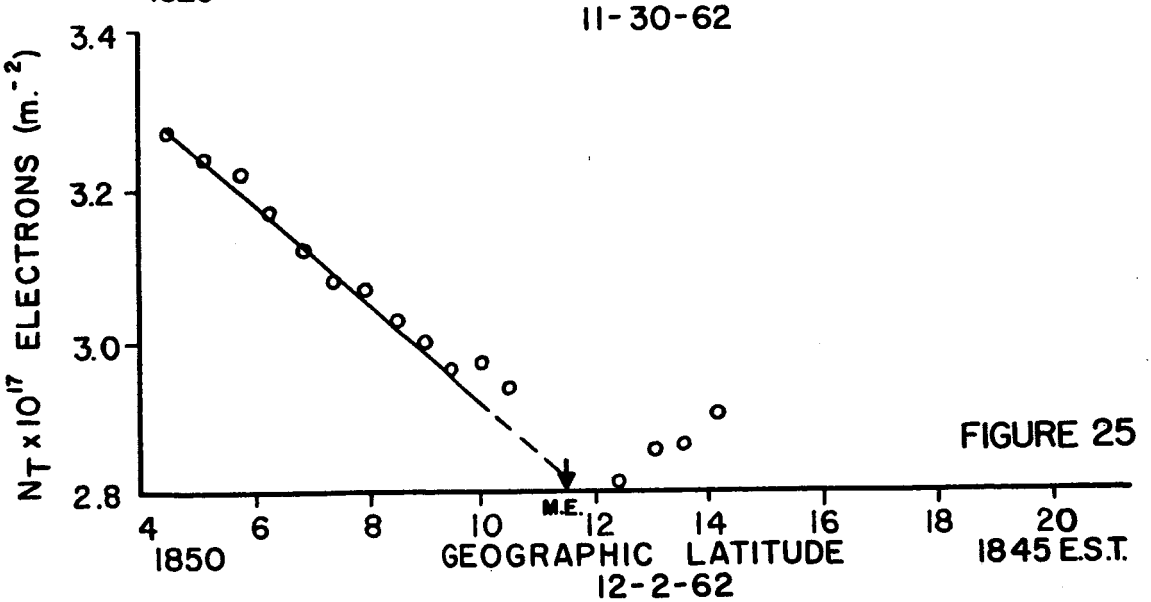

FIGURE 25

TOTAL CONTENT VS LATITUDE

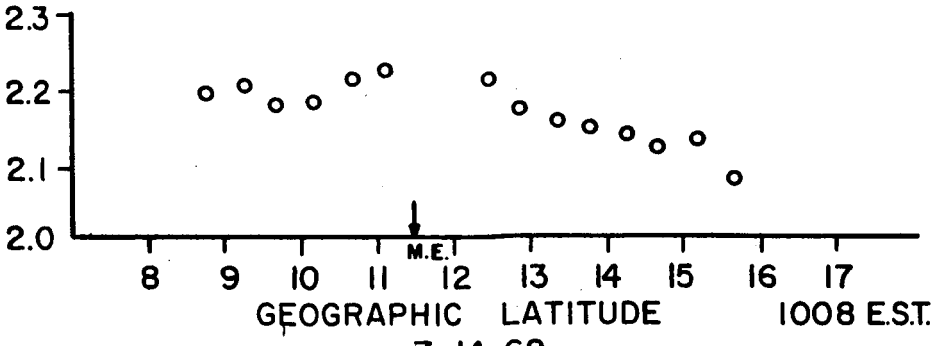

7-14-62

FIGURE 26

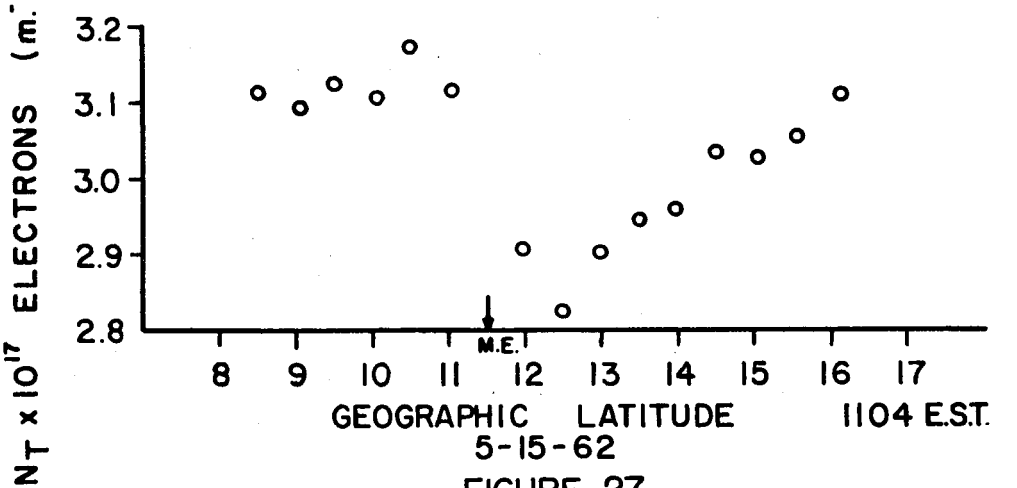

5-15-62

FIGURE 27

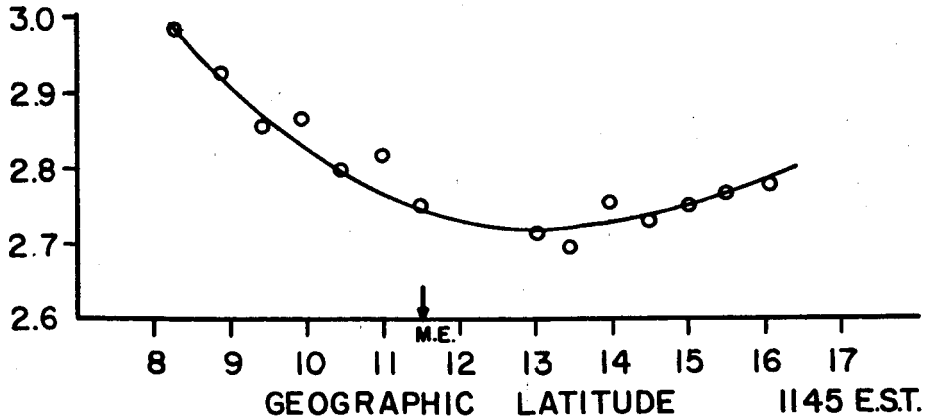

5-9-62

FIGURE 28

CHAPTER 5 - DISCUSSION OF RESULTS

A. Equation of Constraint Calculations

Table II in Chapter four itemizes the results of calculations made with the equation of constraint derived by Chandra and Goldberg. In general approximate agreement is obtained between the scale heights calculated and those from the Harris and Priester model.

A closer look at the data reveals that the calculated scale heights are somewhat less than the expected average based on the Harris and Priester model, especially at the greater heights. There are several possible reasons why better agreement is not obtained. First, at higher altitudes near 700 km scaling of data along field lines becomes increasingly difficult since these field lines have apogees even higher than 700 km. Also increased scatter in the Alouette data introduces greater error at the higher levels.

Secondly, the theory of Chandra and Goldberg is basically for a single constituent ionosphere, while the atmosphere at heights above 400-500 km has a composition which varies rapidly with height, particularly due to the increasingly important amounts

of helium. Helium ions also make up an appreciable proportion of the ionization at these heights. The form of the equation of constraint has not been determined for a multiconstituent ionosphere, and the height derivatives for ionization, calculated from the experimental data, do not necessarily bear the same relationship to the scale height of the neutral atmosphere as for a single constituent.

Also, no consideration of temperature gradients with height is taken into account with Chandra and Goldberg's model. In a recent preprint Goldberg included the effects of a variable electron temperature into the model. An additional term is introduced into the equation of constraint (equation (32)). This term can affect the values of the computed scale heights, but since the temperature changes little above 500 km, one would not expect large changes in the computed scale height averages above this level.

Finally the equation of constraint was derived on the assumption that electron and ion temperatures are equal. Recent measurements at mid-latitudes have shown that during the day the electron temperature in the F region frequently exceeds the ion and neutral temperature by a factor of two.

A similar departure from isothermy might be expected at low latitudes also. The question then arises as to the value of temperature to use in the equation of constraint, or even as to whether the equation is still valid at all.

Many of these difficulties cannot be resolved at this time.

It does seem however that calculations of scale height using the equation of constraint yield values which are not unreasonable and that this may be taken as lending indirect support to its use.

B. Chapman Boundary Condition

Table III and Figure 7 give the results of fitting a Chapman function to the topside of the N-h profiles. Agreement of roughly 15 to 25 per cent is obtained in total content comparison with some tendency for the models to predict low values.

Several points are to be considered. The profile fitting on the topside was done using a constant scale height chosen from Harris and Priester's model of the ionosphere. This scale height was evaluated 50 km above the height of "N maximum" so as to represent a mean scale height

of the topside. The scale height in the ionosphere actually varies with altitude. Effects of variable electron and ion temperatures, acceleration of gravity varying with height and the change of composition with height contribute to this variation.

What is tested by these comparative data is principally whether the model gives an electron density which falls off at about the right rate above the level of peak density. Most of the ionization is contained within a few scale heights on either side of the peak density level, and relatively little is contributed to the electron content by the tail of the distribution. Consequently the detailed form of the model profile cannot be verified by this method. The generally good agreement seen in the Table may be taken to mean that the use of a Chapman topside profile using the scale height of atomic oxygen evaluated about one scale height above the peak of the layer gives a reasonable model of the equatorial electron density profile in the upper F layer.

Under these circumstances and with these data, the use of more sophisticated models, e.g. the scale height gradient model of Chandra (1963); which may produce better agreement with experiment through

choice of additional parameters for particular records, cannot be justified.

The height of "N maximum" determined from the bottomside profile, is subject to some uncertainty, and this in term leads to uncertainty in the height at which the model topside profile is started. Typically an error of 30 km in $h_{max.}$ will lead to a 10% error in electron content, and there may be some scatter in the data from this cause. This effect is evident from Figure 7 for the record of 2/16/62 at 1924 EST. This was a magnetically disturbed day. Considerable scatter of data near the critical frequency prevented a reliable calculation of the height of "N max" from the ionogram. This is evident from the comparison with the Faraday Rotation data in Table II. The total content measured is greater than experimental results by a factor greater than two, and in fact the profile would have to fall to zero density immediately above the supposed peak in order to produce agreement with the experimental data.

The question of isothermy between ions and electrons arises here also as it did in the first section of this chapter. If the electron temperature is indeed high as has been claimed by Spencer, Brace,

and Corrigan (1962), then the use of a larger value than the ion temperature used here might be suggested. However this temperature cannot be raised more than about 50% without producing discrepancies with observation in the other direction. It can be seen from Figure 7 that the Chapman model used here gives a rather better fit toward evening when isothermy should be more nearly established. To interpret this diurnal trend as strong evidence for a departure from isothermy during the day is not warranted however, in view of the uncertainty concerning the formal description of the equatorial ionosphere profile.

C. Total Content Variation with Latitude

Table III lists the results of the comparison of total electron content variation with latitude as predicted from Chandra and Goldberg's model with the Faraday Rotation data. In comparing the data a few points must be kept in mind. First the theoretical predictions are claimed to be valid to 100 km below the height of "N max". The total electron content given by the Faraday Rotation method represents the entire height range from the earth to the satellite. Hence comparing the data directly, no account is taken of

the bottomside geomagnetic anomaly.

In general the change in total content predicted from the theoretical model is large compared to the Faraday data by a factor of about three. An even greater discrepancy would be expected if a theoretical model for the bottomside anomaly were included. At the present time no theory is available for the bottomside and hence prohibits full comparison between theory and experiment.

An important point to note is the effect of vertical drift of ionization on the theoretical model. Chandra and Goldberg use a Chapman like boundary condition in their model. One may expect that the profile at the equator is a result of a mixture of processes of production, loss and vertical and horizontal (to field lines) diffusion. But no effect of vertical drift is included in the theory of Chandra and Goldberg which extends the equatorial profile to other latitudes except through the boundary condition. The manner in which vertical drift varies with latitude near the magnetic equator is not known at the present time.

A recent article by Bramley and Peart (1964) predicts some of the possible effects of vertical

drift on the anomaly. Basically vertical drift is treated as a perturbation to the case of zero vertical drift discussed by Rishbeth, Lyon and Peart (1963). The inclusion of vertical drift explicitly in the continuity equation resulted in an increased electron density at constant heights compared to Rishbeth, Lyon and Peart's calculations. These increased values of electron density are also moved to greater latitudes and to slightly higher altitudes compared to the earlier work, and the equatorial troughs in "N max" and electron content are deepened from 5% to 50%, and from 5% to about 30% respectively for the particular model considered. The inclusion of vertical drift appears to have an important role in the description of the geomagnetic anomaly.

In view of Bramley and Peart's article there may seem to be some disagreement with Chandra and Goldberg's model on the basis of the calculations made here. These show high changes in total electron content for the theoretical model, and one may expect even higher increases if vertical drift is incorporated. What effect vertical drift has on the model is uncertain since it is partially incorporated in the boundary condition.

A feature predicted by Chandra and Goldberg's model, consistent with experiment, is the general shape of the curves of total content variation with latitude. Figures 8 and 9, which have been computed from the Chandra and Goldberg model, provide a general means of comparison with the shapes of the experimental curves of total electron content vs latitude. Roughly speaking the experimental total content curves are "V-shaped"; between 2 and 7 degrees magnetic latitude on each side of the magnetic equator, the curves are nearly straight lines. These general features are in reasonable agreement with the predicted curves.

D. Behavior of the Total Electron Content with Latitude During Magnetically Disturbed Periods

To illustrate a trend in Table IV it is useful to examine the total electron content variation with latitude in two sets of bracketed days. The first set consists of the two days prior to a magnetic disturbance. If a total content record falls on the day of the disturbance but prior to, or within one hour following the onset of the storm, it is included in this first set. The two days following a magnetic disturbance comprise the second set. The days on which no total content record

are available will not be counted in the statistics derived from Table IV. Table V gives a summary of the total content behavior with latitude for these sets of days. The symbol A means the anomaly is present. Days with "?" in table IV are also considered as having no anomaly present.

TABLE V - SUMMARY OF TOTAL CONTENT VARIATION WITH LATITUDE BEHAVIOR PATTERN

Two days Prior to Disturbance	A	no. A	Two Days following Disturbance	A	no. A
11/5/61	*		11/8/61		*
11/6/61	*		11/17/61		*
11/16/61	*		12/7/61	*	
3/4/62	*		2/15/62		*
4/8/62		*	2/16/62	*	
4/9/62	*		3/5/62	*	
4/19/62	*		3/6/62	*	
4/20/62	*		3/7/62	*	
9/18/62	*		4/10/62	*	
11/29/62		*	4/21/62	*	
12/2/62	*		9/19/62		*
12/3/62	*		11/30/62		*
			12/4/62		*
			12/5/62		*

From Table V it is noted that for two day periods prior to magnetic disturbances two out of the twelve days have no anomaly present. In the two day periods following magnetic disturbances seven out of fourteen days have no anomaly present. These statistics imply that the anomaly in total content has a 50% chance of disappearance following a magnetic disturbance.

This general behavior is illustrated in the following sequences of records. Figures 15 through 17 illustrate the total content variation with latitude near the storm day, 11/17/61. On the 16th the anomaly is clearly distinct whereas on the 17th and 19th no anomaly appears. Figures 23 through 25 illustrate the behavior around 11/30/62. On the 29th and 30th no anomaly appears. On 12/2/62 the anomaly is present once more. Figures 18 through 22 illustrate the behavior on days surrounding 4/10/62. On the 7th the anomaly is distinct and on the 8th the data is uncertain. On the 9th and 10th the anomaly is once again distinct. On the 12th the anomaly is distinct north of the magnetic equator. In this sequence of records the anomaly apparently persists on the days following the disturbance.

The theories discussed in this paper do not account for magnetically disturbed days. From the experimental viewpoint some indications are available. J. W. King et al. (1963) gives a description for the topside equatorial ionosphere on magnetically disturbed days. On the topside the electron density variation with latitude is less pronounced on magnetically disturbed days, i.e. curves similar to Figure 2 in Chapter I are flatter, and the angular peaks are spread further apart than usual. Qualitatively speaking, from the observations one would expect a general flattening of the total electron content variation with latitude.

E. Daily Appearance of Anomaly in Total Content

Figures 26 through 28 illustrate typical behavior of the first order total content in the morning. At ten o'clock the anomaly is not present. At eleven it is partially developed and near noon it is well developed. These figures shed some insight in to what times the anomaly in total content appears.

It is not possible to observe the appearance of the anomaly on any particular day, since only one satellite record is available each day.

Consequently only an average time of appearance can be found, based on records taken over a period of several days, and any variation of this time with solar activity, etc., cannot be determined.

In the evening no approximate times could be set for the disappearance of the anomaly. A few records indicated the anomaly present as late as 2330 hours, but in other cases it had apparently disappeared much earlier.

F. Statement of the Problem

It is the purpose of this paper to analyze the existing theories and models describing the geomagnetic anomaly and to examine them in relation to available experimental data obtained from:

1) Measurements of total electron content variation with latitude over Huancayo, Peru, using satellite beacon methods.

2) Topside electron density profiles calculated from some Alouette topside sounder data over Singapore.

A study is also made of the behavior of the anomaly in total electron content during magnetically disturbed periods.

G. Summary and Conclusion

In this work a summary of the theories describing the geomagnetic anomaly were presented. The model of Chandra and Goldberg was used in an attempt to relate theory with experiment. The calculations using Chandra and Goldberg's equation of constraint led to reasonable values of scale heights inferring indirect support to the use of the equation. The Chapman boundary condition was shown to be a reasonable choice, in that when it was applied using scale heights derived from an independent atmospheric model, the predicted electron content agreed generally to better than 25% with the content computed experimentally by Faraday Rotation methods. The predicted variation of electron content with magnetic latitude has a similar "V" shape to that found experimentally, but the rate of change of content with latitude is too large by about a factor of three.

Chandra and Goldberg's model is derived basically on <u>effect</u> and not on causal physical principles. A boundary condition is assumed at the magnetic equator and the effect of diffusion along field lines on this boundary condition is derived. The recent publication by Bramley and

Peart also appears to lead to a model which is reasonably consistent with the main features of the geomagnetic anomaly. Their solutions result from numerical integration of the continuity equation but the approach is more "causal" in the physical sense. The Bramley and Peart results however are not derived in an analytic form, and which includes the physical parameters of the problem. Comparison with experimental data can be done only by numerical integrations of their equation with various values of the parameters included. This was not possible in view of the recent date of publication.

The calculations in this paper do not present a complete varification of Chandra and Goldberg's model. They do indicate however that it is a reasonable working model describing the geomagnetic anomaly.

The study of total electron content behavior with latitude during magnetically disturbed periods indicated that while an equatorial anomaly is almost always present during the afternoon on quiet days, on days following a local magnetic storm its probability of occurrence drops to about one-half.

ACKNOWLEDGEMENTS

The guidance of Dr. W. J. Ross in this study is deeply appreciated. The Computress Staff of the Ionosphere Research Lab assisted in numerous calculations. The magnetic field components and ionospheric point calculations were computed by Goddard Space Flight Center. Ephemeris for Transit 4A was supplied by the Applied Physics Lab, Johns Hopkins, and numerous bottomside profiles were furnished by C. R. P. L. This study could not have been possible without the cooperation of Instituto Geofico del Peru in obtaining numerous Faraday Rotation records. This work was supported by The National Aeronautics and Space Administration under Grant NsG-114-61.

BIBLIOGRAPHY

Appleton, E. (1947); Sci. 106 p. 17
(1950); J.A.T.P. 1 pp. 106-113
(1954); J.A.T.P. 5 pp. 349-351.

Bramley, E. M., Peart, M. (1964) J.G.R. 69 pp 4609-4620

Blumle, L. J. (1961) Ionospheric Research Sci. Report No. 156 March 1, Pa. State Univ.

Chandra, S., (1963) J.G.R. 68 1937-1942

Chandra, S., Goldberg, R. A. (1964) J.G.R. 69 pp. 3187-3197

Croom, S., Robbins, A., Thomas, J. (1959) Nature 184 p. 2003

Duncan, R. A. (1960) J.A.T.P. 18 pp 89-99

Goldberg, R. A., N.A.S.A. preprint X-615-64-279

Goldberg, R. A., Kendall, P. C. & Schmerling, E. R. (1964) J.G.R. 69 pp 417-427

Goldberg, R. A., Schmerling, E. (1962) J.G.R. 67 pp 3813-3815
(1963) J.G.R. 68 pp 1927-1936

Harris, I., & Priester, W., (Aug. 1962) N.A.S.A. Tech. note TND-1444

Kendall, P. C., (1962) J.A.T.P. 24 pp 805-811
(1963) J.A.T.P. 25 pp 87-91

King, J. W. et al. (1963) Radio Research Station document R.R.S. IM 112

Lyon, A. J. (1963) J.G.R. 68 pp 2531-2540

Martyn, D. F. (1959) Proc. I.R.E. 47 pp 147-155

Ratcliffe, J. (1956) J.A.T.P. 8 pp 260-269

Rishbeth, M., Lyon, A. J., & Peart, M. (1963) J.G.R. 68 pp 2559-2569

Ross, W. J. (1964) Ionospheric Research Sci. Report No. 156 March 1, Pa. State Univ.

Spencer, N., Brace, L., Corrigan, G. (1962) J.G.R. 67 pp 157-175